



## Calhoun: The NPS Institutional Archive

---

Theses and Dissertations

Thesis Collection

---

1985

The character of observed porosity and its possible effects on rolling contact fatigue life of M-50 steel.

Perry, James L.

---

<http://hdl.handle.net/10945/21191>



Calhoun is a project of the Dudley Knox Library at NPS, furthering the precepts and goals of open government and government transparency. All information contained herein has been approved for release by the NPS Public Affairs Officer.

**Dudley Knox Library / Naval Postgraduate School  
411 Dyer Road / 1 University Circle  
Monterey, California USA 93943**

<http://www.nps.edu/library>







DUDLEY KNOX LIBRARY  
NAVAL POSTGRADUATE SCHOOL  
MONTEREY, CALIFORNIA 93943





# NAVAL POSTGRADUATE SCHOOL

## Monterey, California



# THESIS

THE CHARACTER OF OBSERVED POROSITY AND ITS  
POSSIBLE EFFECTS ON ROLLING CONTACT  
FATIGUE LIFE OF M-50 STEEL

by

James L. Perry

March 1985

Thesis Advisor:

T. R. McNelley

Approved for public release; distribution is unlimited

T224134



UNCLASSIFIED

SECURITY CLASSIFICATION OF THIS PAGE (When Data Entered)

REPORT DOCUMENTATION PAGE		READ INSTRUCTIONS BEFORE COMPLETING FORM
1. REPORT NUMBER	2. GOVT ACCESSION NO.	3. RECIPIENT'S CATALOG NUMBER
4. TITLE (and Subtitle) The Character of Observed Porosity and Its Possible Effects on Rolling Contact Fatigue Life of M-50 Steel		5. TYPE OF REPORT & PERIOD COVERED Master's Thesis; March 1985
7. AUTHOR(s) James L. Perry		6. PERFORMING ORG. REPORT NUMBER
9. PERFORMING ORGANIZATION NAME AND ADDRESS Naval Postgraduate School Monterey, California 93943		8. CONTRACT OR GRANT NUMBER(s)
11. CONTROLLING OFFICE NAME AND ADDRESS Naval Postgraduate School Monterey, California 93943		10. PROGRAM ELEMENT, PROJECT, TASK AREA & WORK UNIT NUMBERS
14. MONITORING AGENCY NAME & ADDRESS (if different from Controlling Office)		12. REPORT DATE March 1985
		13. NUMBER OF PAGES 71 pages
		15. SECURITY CLASS. (of this report) Unclassified
		15a. DECLASSIFICATION/ DOWNGRADING SCHEDULE
16. DISTRIBUTION STATEMENT (of this Report)  Approved for public release; distribution in unlimited		
17. DISTRIBUTION STATEMENT (of the abstract entered in Block 20, if different from Report)		
18. SUPPLEMENTARY NOTES		
19. KEY WORDS (Continue on reverse side if necessary and identify by block number) Rolling Contact Fatigue, M-50 Steel, Thermomechanical Processing, Residual Carbides, Porosity, Void Size Distribution, Bearings, Void Origin Model		
20. ABSTRACT (Continue on reverse side if necessary and identify by block number)  AISI M-50 steel was warm-rolled at 750°C (1382°F). Samples of both warm-rolled and as-received (spheroidized annealed) M-50 were austenitized at 1036°C (1897°F) for various times and subsequently tempered. The heat treated samples were subjected to rolling contact fatigue (RCF) testing. In all cases prior warm-rolling degraded the RCF life at both the L <sub>10</sub> and L <sub>50</sub> levels.		

DD FORM 1473  
1 JAN 73

EDITION OF 1 NOV 65 IS OBSOLETE

S/N 0102-LF-014-6601

UNCLASSIFIED

1 SECURITY CLASSIFICATION OF THIS PAGE (When Data Entered)



20. (Continued)

Scanning electron microscopy was used to examine the microstructure of the as-received and warm-rolled material between 4000X and 10,000X magnification. Voids in the 0.3  $\mu\text{m}$  to 2.2  $\mu\text{m}$  range were documented within the microstructures. It was found that warm-rolling increased geometric mean of the void size in the transverse direction from 0.485  $\mu\text{m}$  to 0.768  $\mu\text{m}$ , and from 0.629  $\mu\text{m}$  to 0.882  $\mu\text{m}$  in the longitudinal direction.

It is thought that the increase in the void diameters accounts for the decrease in RCF performance of warm-rolled M-50. The degraded RCF performance is due to both the increase in mean void diameter and the increase in larger sized voids that accompany warm rolling. A qualitative model was developed to account for the origin of voids in as-received material and for the increase in void diameter in warm-rolled material.

Approved for public release; distribution is unlimited

The Character of Observed Porosity and Its Possible Effects  
on Rolling Contact Fatigue Life of M-50 Steel

by

James L. Perry  
Lieutenant, United States Navy  
B.S., Auburn University, 1977

Submitted in partial fulfillment of the  
requirements for the degree of

MASTER OF SCIENCE IN MECHANICAL ENGINEERING

from the

NAVAL POSTGRADUATE SCHOOL  
March 1985

## ABSTRACT

AISI M-50 steel was warm-rolled at 750°C (1382°F). Samples of both warm-rolled and as-received (spheroidized annealed) M-50 were austenitized at 1036°C (1897°F) for various times and subsequently tempered. The heat treated samples were subjected to rolling contact fatigue (RCF) testing. In all cases prior warm-rolling degraded the RCF life at both the  $L_{10}$  and  $L_{50}$  levels.

Scanning electron microscopy was used to examine the microstructure of the as-received and warm-rolled material between 4000X and 10,000X magnification. Voids in the 0.3  $\mu\text{m}$  to 2.2  $\mu\text{m}$  range were documented within the microstructures. It was found that warm-rolling increased geometric mean of the void size in the transverse direction from 0.485  $\mu\text{m}$  to 0.768  $\mu\text{m}$ , and from 0.629  $\mu\text{m}$  to 0.882  $\mu\text{m}$  in the longitudinal direction.

It is thought that the increase in the void diameters accounts for the decrease in RCF performance of warm-rolled M-50. The degraded RCF performance is due to both the increase in mean void diameter and the increase in larger sized voids that accompany warm rolling. A qualitative model was developed to account for the origin of voids in as-received material and for the increase in void diameter in warm-rolled material.

## TABLE OF CONTENTS

I.	INTRODUCTION . . . . .	9
II.	EXPERIMENTAL PROCEDURE . . . . .	13
	A. INITIAL PREPARATION OF MATERIAL . . . . .	13
	B. WARM ROLLING . . . . .	13
	C. FINAL HEAT TREATING . . . . .	14
	D. ROLLING CONTACT FATIGUE TESTING . . . . .	16
	E. MICROSCOPY . . . . .	19
III.	RESULTS AND DISCUSSION . . . . .	24
	A. ROLLING CONTACT FATIGUE TESTING . . . . .	24
	B. POROSITY CHARACTERIZATION . . . . .	37
	C. VOID FORMATION . . . . .	44
IV.	CONCLUSIONS AND RECOMMENDATIONS . . . . .	53
	A. CONCLUSIONS . . . . .	53
	B. RECOMMENDATIONS . . . . .	53
	APPENDIX A . . . . .	55
	APPENDIX B . . . . .	56
	APPENDIX C . . . . .	66
	LIST OF REFERENCES . . . . .	69
	INITIAL DISTRIBUTION LIST . . . . .	71



## LIST OF FIGURES

2.1	Disk-Rod Tester Used by Wright Aeronautical Laboratory. RCF Rod is Mounted Between the Disks as Arrow Indicates . . . . .	18
2.2	Schematic View of the Ball and Rod Arrangement in Ball-Rod Tester . . . . .	19
2.3	Ball-Rod Tester Used by Wright Aeronautical Laboratory. RCF Rod is Shown (Arrow) Mounted on Machine . . . . .	20
2.4	Void Size Distribution of As-Received Material in Longitudinal Direction. Histogram Represents Raw Data, Dotted Curve Represents Curve Fit Through Grouped Data . . . . .	23
3.1	Weibull Plot for Specimen F1 (As-Received) Compared to Standard M-50 Material. F1 was Austenitized at 1106°C for 5 Minutes . . . . .	26
3.2	Weibull Plot for Specimen N (Warm-Rolled) Compared to Standard M-50 Material. N was Austenitized at 1036°C for 5 Minutes . . . . .	28
3.3	Weibull Plot for Specimen D (Warm-Rolled) Compared to Standard M-50 Material. D was Austenitized at 1036°C for 1 Minute . . . . .	30
3.4	Weibull Plot for Specimen F2 (Warm-Rolled) Compared to Standard M-50 Material. F2 was Austenitized at 1036°C for 2 Minutes . . . . .	31
3.5	Weibull Plot for Specimen G (As-Received) Compared to Standard M-50 Material. G was Austenitized at 1036°C for 2 Minutes . . . . .	33
3.6	RCF Life Summary. Warm Rolling is Believed to Have Increased Void Dimensions Causing RCF to be Degraded . . . . .	35
3.7	Comparison of Void Size Distributions, Transverse Direction . . . . .	39

3.8	Comparison of Void Size Distributions, Longitudinal Direction . . . . .	40
3.9	SEM Micrographs, As-Received Material. A is from the Transverse Direction, B is from the Longitudinal Direction . . . . .	42
3.10	SEM Micrographs, Warm-Rolled Material. A is from the Transverse Direction, B is from the Longitudinal Direction . . . . .	43
3.11	SEM Micrographs, Bearing Race . . . . .	45
3.12	Conceptual Model for Void Formation . . . . .	47
3.13	Fractured Carbides Within As-Received M-50 . . . . .	50
3.14	Carbide Pieces Strewn Through Warm-Rolled Microstructures . . . . .	51

## ACKNOWLEDGEMENT

My sincerest thanks go to my thesis advisor, Professor Terry R. McNelley, who kept the "big picture" at all times and was able to offer guidance when it was most needed. Mr. Tom Kellogg and Mr. Tom McCord of NPS were especially helpful with technical matters. Mr. Chris Patton of Stanford's Hopkins Marine Lab provided training to accomplish the required SEM work. Mr. Ron Dayton of the Air Force Wright Aeronautical Laboratory shepherded the RCF testing in a timely fashion and was always only a phone call away. Special thanks go to my fellow slugs who were merely classmates two years ago and are now exceptional friends.

## I. INTRODUCTION

The need to extend rolling contact fatigue life of gas turbine bearing materials has provided the impetus for this study of AISI M-50 steel. Presently, M-50 is widely used as a bearing material for current generation gas turbines. This widespread use is due to the ability of M-50 to retain its hardness at elevated temperatures and its ability to resist wear. These two characteristics are required for the alternating Hertzian stress environment to which rolling element bearings are subjected.

At this point in time, M-50 satisfactorily meets the demands for bearing rolling contact fatigue life for gas turbines in current use. Incremental improvements in gas turbine designs and gas turbine blading materials are pushing future turbine DN ratings toward  $3.0 \times 10^6$  vice the present day  $2.0 \times 10^6$ . DN is a turbine rating obtained from the product of a shaft's diameter in mm and the shaft's speed in RPM. Increasingly efficient turbine designs will thus require that a bearing material possess a longer fatigue life than is presently required.

One approach to this problem of extended fatigue life is to modify the microstructure of the currently used M-50 steel with the intent of delaying fatigue crack initiation



and/or reducing the rate at which fatigue cracks propagate through the material. Other approaches to the problem included surface treatments, such as surface carburization of M-50 steel, or outright replacement of M-50 with a superior material.

Sherby, et. al., [Ref. 1] has shown that warm rolling, a form of thermomechanical processing, refined the grain structure of a commercial eutectoid steel. Warm rolling consisted of rolling the steel at a temperature of 600°C to 650°C and attaining a final true strain of up to 2.0. This produced a finely spheroidized pearlite within the eutectoid steel microstructure.

Following Sherby's lead, McNelley, et. al., [Ref. 2] warm rolled AISI 52100 steel and found that the procedure gave a fine dispersion of carbides and decreased final grain size. An increase in yield strength was attributed to these two factors.

The initial step in development of a warm rolling procedure for M-50 was taken by Larson. Larson [Ref. 3] found that warm rolling of M-50 steel in the range of 650°C to 750°C similarly produced finely dispersed soluble carbides but did little to refine the size of the more massive residual carbides found in this variety of steel. The specific results of warm rolling are production of a microstructure of refined carbides in a fine-grained

ferrite. As such, the warm-rolled microstructure is a much refined version of the as received material and must still be subjected to a hardening treatment. As-received M-50 is in a spheroidized anneal condition and possesses a grain size on the order of 16-20  $\mu\text{m}$  with soluble carbides on the order of 2-3  $\mu\text{m}$ . By comparison, warm-rolled M-50 possesses a grain size on the order of 1-3  $\mu\text{m}$  and soluble carbides on the order of 0.1-0.2  $\mu\text{m}$ . Residual carbides are on the order of 5-10  $\mu\text{m}$  in both the warm-rolled and as-received conditions.

Following Larson's work, Bres [Ref. 4] was able to carry out hardening experiments and illustrate the effect of warm rolling upon the hardening response of M-50. It was found that warm-rolled M-50 could be austenitized at a lower temperature than as-received material, yet attain similar hardness. This reduction of austenitizing temperature was attributed to the refined soluble carbides being able to deliver more carbon to the matrix. Naturally, the higher the carbon content of the matrix the greater the hardness of the steel.

With the results of Larson's and Bres' work, Butterfield [Ref. 5] initiated rolling contact fatigue testing of warm-rolled M-50. The warm rolling techniques developed by Larson were adapted to a larger specimen size to permit rolling to a final bar shape. This was necessitated by the

requirement to fabricate RCF test rods from the warm-rolled material. The hardening sequences used by Bres were likewise adapted to the larger specimen size used for RCF testing. The data generated by Butterfield showed that M-50 material subjected to TMP did not improve RCF life over material that had not been subjected to warm rolling when both materials conditions were hardened in the same manner. It was also noted that overheating of the warm-rolled material had taken place; a five-minute austenitization period coarsened the microstructure of warm-rolled material to the point that it could scarcely be differentiated from that of hardened as-received material. Furthermore, his study raised the possibility that voids found within the M-50 microstructure could be a controlling factor in the RCF life of M-50 specimens. These voids were found in the vicinity of residual carbides found in M-50 in both the as-received condition (spheroidized anneal) and the warm-rolled condition.

This study was undertaken subsequent to the work of Butterfield and began with two distinct goals in mind. The first is to complete RCF testing over a wider range of heat treating conditions than had been previously accomplished. The second is to characterize the porosity observed in M-50 and to evaluate the effect of warm rolling upon the void size distribution in the material.

## II. EXPERIMENTAL PROCEDURE

### A. INITIAL PREPARATION OF MATERIAL

Initial preparation of M-50 stock followed the procedures outlined by Butterfield [Ref. 5: p. 16]. VIM-VAR M-50 stock material used in this experiment was obtained from the manufacturer in the shape of 1.75 inch (44.45 mm) diameter rod in a spheroidize-anneal condition. Six inch (157.4 mm) lengths of the material were cut and initially heated to 850°C for two hours. Following this preheat the material was transferred to a furnace at 1150°C and held there for an additional two hours. The material was furnace quenched at 620°C for three minutes and then allowed to air cool. At all times during the thermal cycling the material was wrapped in a nickel foil packet. Additionally, a small piece of titanium sponge was placed within the packet to act as an oxygen scavenger. These steps were taken to minimize any surface decarburization of the M-50 stock prior to the start of thermomechanical processing.

### B. WARM ROLLING

Following the initial austenitizing treatment outlined above the lengths of M-50 were delivered to the Lawrence Berkeley Laboratories, Berkeley, California for the warm rolling phase of the processing procedure. There the M-50



rods were initially flattened on four sides on a two-high flat mill after being heated to  $700^{\circ}\text{C}$  ( $1292^{\circ}\text{F}$ ) in an electrically-fired box furnace. This was required to establish a semi-square cross section to allow subsequent rolling in a two-high bar mill. Rolling in the bar mill continued until the bar had been reduced to 0.600 inches (15.2 mm) on a side. Following each pass through either of the above mills the M-50 was returned to the furnace in order to maintain the deformation temperature as close as possible to  $700^{\circ}\text{C}$  ( $1292^{\circ}\text{F}$ ). Thus, the warm rolling reduced the cross sectional area of the material from 2.41 square inches ( $15.55\text{ mm}^2$ ) to 0.360 square inches ( $2.32\text{ mm}^2$ ), a true strain of 1.90.

#### C. FINAL HEAT TREATING

Following warm rolling, the now bar shaped M-50 pieces were cut into  $4.0 \pm 0.1$  inch ( $102 \pm 2$  mm) lengths and machined to a  $0.395 \pm 0.005$  inch ( $10.0 \pm 0.05$  mm) diameter rod. Samples of this size were used in the final phase of heat treating. This phase consisted of austenitizing samples of warm-rolled material and as-received material for like temperatures and time periods. For each austenitizing temperature and time selected, a sample of both as-received material and warm-rolled material were used. This was done for the sake of comparison when rolling contact fatigue testing was later carried out as well as for the sake of

microstructural and hardness comparisons. A total of five distinct austenitizing temperature and time combinations were prepared for rolling contact fatigue (RCF) testing. These are presented in Appendix A along with the combinations prepared by Butterfield. Austenitizing times of one, two, and five minutes were used for the specimens of this study. These times were chosen to evaluate the overheating of those test rods that were austenitized in prior work. This final austenitizing treatment was carried out by a commercial heat treating firm due to the lack of necessary equipment at NPS, Monterey.

The austenitizing process was carried out in three steps: preheat, austenitizing, and quench. All three steps were conducted in a molten salt bath, with preheating carried out at  $845^{\circ}\text{C}$  ( $1553^{\circ}\text{F}$ ) for four to five minutes and the equalizing quench was followed by air cooling. Tempering of the specimens was carried out several days later.

The tempering process consisted of five steps, with each step of two hours duration. Initially the austenitized samples were given a sub-zero cycle in frozen acetone at  $-90^{\circ}\text{C}$  ( $-130^{\circ}\text{F}$ ) to  $-95^{\circ}\text{C}$  ( $-139^{\circ}\text{F}$ ). Following this the samples were given a cycle at  $540^{\circ}\text{C}$  ( $1004^{\circ}\text{F}$ ) in an electric box furnace. Next the samples were cycled through the frozen acetone treatment again. This was followed by two

consecutive cycles at 540°C (1004°F) in the electric box furnace. After each step the samples were allowed to equalize with room temperature before proceeding on to the next step in the tempering scheme.

#### D. ROLLING CONTACT FATIGUE TESTING

Following the five step tempering cycle detailed above, all samples were forwarded to the Naval Air Propulsion Center (NAPC), Trenton, New Jersey for final surface grinding. The RCF rods were ground to a surface finish of four to eight microinches RMS and a final diameter of 0.375 + 0.002 inches ( $9.53 \pm 0.05$  mm).

Once in their final form the samples were shipped to the Air Force Wright Aeronautical Laboratory, Wright-Patterson AFB, Dayton, Ohio for actual RCF testing. It should be noted that the RCF tests documented below are accelerated failure tests in that the applied loads are several times larger than the normal environmental loads experienced by fabricated bearings.

Disk-rod RCF testing was carried out in the manner described in detail by Popgoshev and Valori [Ref. 6] for samples N and Fl. In these tests the disk-rod tester developed by General Electric in the mid 1970's was used. This rig applies a maximum Hertzian stress of 700 ksi (4826 MPa) to the test rod, while it is being turned at 12,500 rpm by a small electric motor. In turn the test rod

drives two disks that are seven to eight inches in diameter and made of a similar bearing type material. These two disks are loaded by a calibrated load cell and transfer a Hertzian stress to the test rod. Figure 2.1 shows a photo of the disk-rod tester with a test rod mounted between the disks.

The next four samples tested, D, G, and F2, were tested within a somewhat different manner. For these samples a ball-rod RCF tester was used as described by Glover [Ref. 7].

The same specimen size is used as in the G.E. tester used for samples N and F1. However, as the name implies the ball-rod tester uses three balls around the RCF specimen to apply a load and establish the wear tracks. The three balls are  $0.500 \pm 0.002$  inches ( $12.70 \pm 0.05$  mm) in diameter and made of AISI 52100 Grade-24 steel with a surface finish of 3.5 microinches. Lubrication is supplied at the rate of 10 drops per minute with Mil-L-7808 used as the lubricant. As in the disk-rod RCF tests a vibration sensor causes the test to terminate once a spall or fatigue crack develops within the wear track. Applied Hertzian stress is somewhat higher with this tester, 786 ksi (5419 MPa) vice 700 ksi (4826 MPa) while rotational speed is lower, 3600 rpm vice 12,500. Figure 2.2 shows the schematic relationship between balls and rod, while Figure 2.3 is a photo of the ball-rod tester



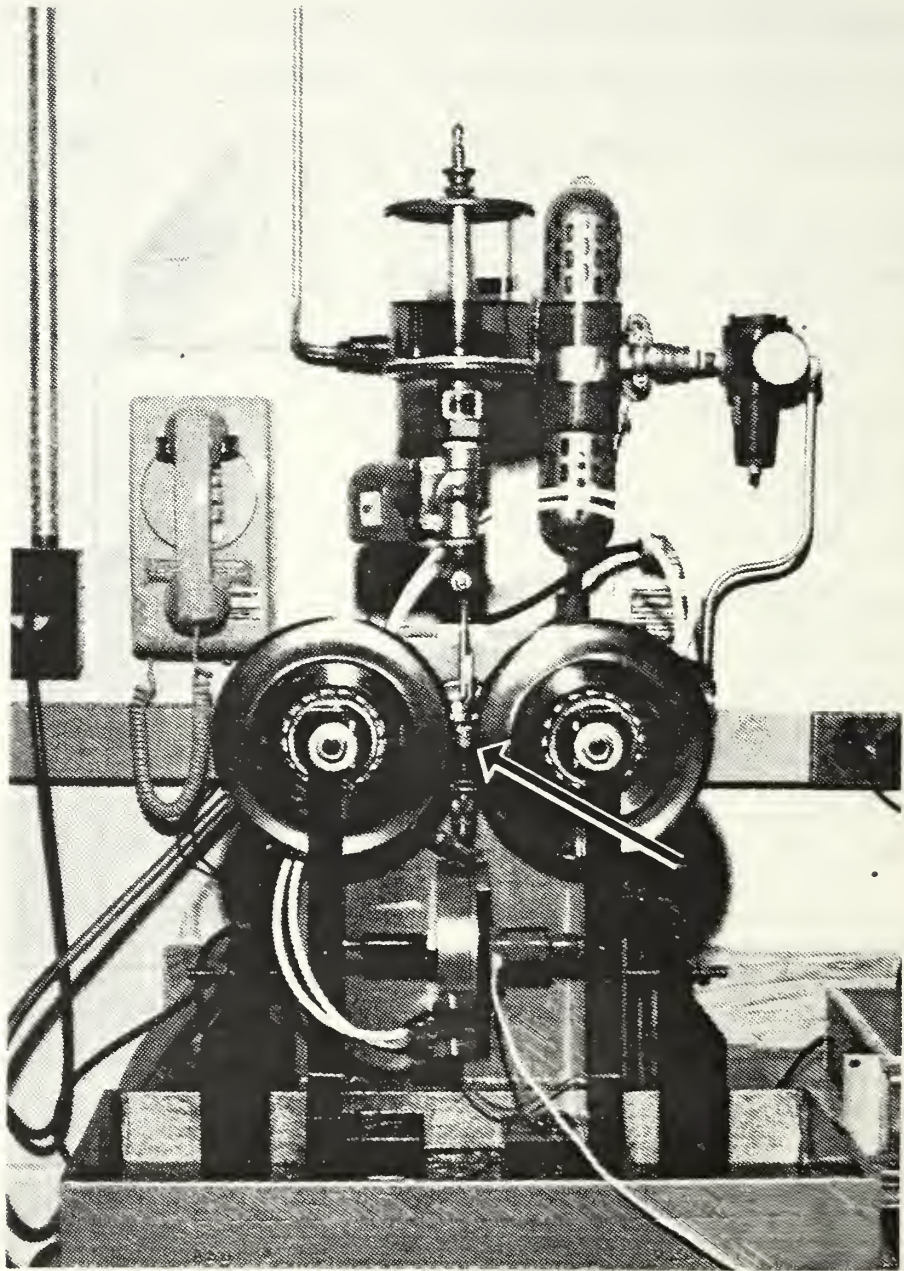


Figure 2.1. Disk-Rod Tester Used by Wright Aeronautical Laboratory. RCF Rod is Mounted Between the Disks as Arrow Indicates.

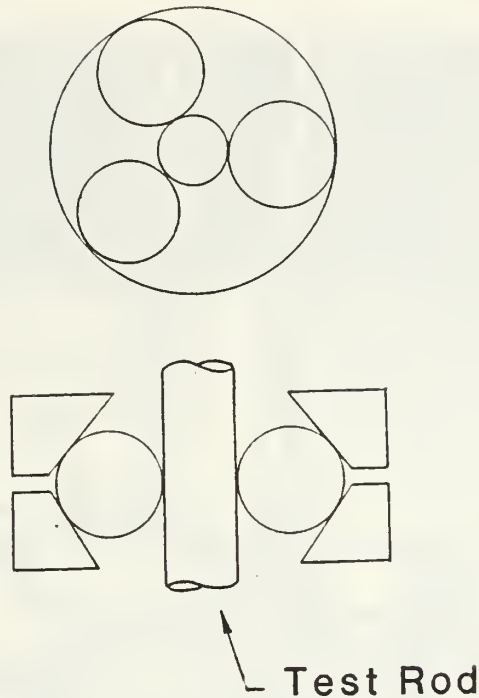


Figure 2.2. Schematic View of the Ball and Rod Arrangement in Ball-Rod Tester

with a rod in the test position. The ball-rod tester offers an economic advantage over the disk-rod tester in that "off the shelf" balls can be used rather than machined disks for contact loading.

#### E. MICROSCOPY

Optical microscopy was conducted with a Zeiss Photomicroscope and optical micrographs were recorded on Kodak Technical Pan film. Scanning electron microscopy was conducted with a Hitachi scanning electron microscope and SEM micrographs were recorded on Polaroid Type 55 film. All



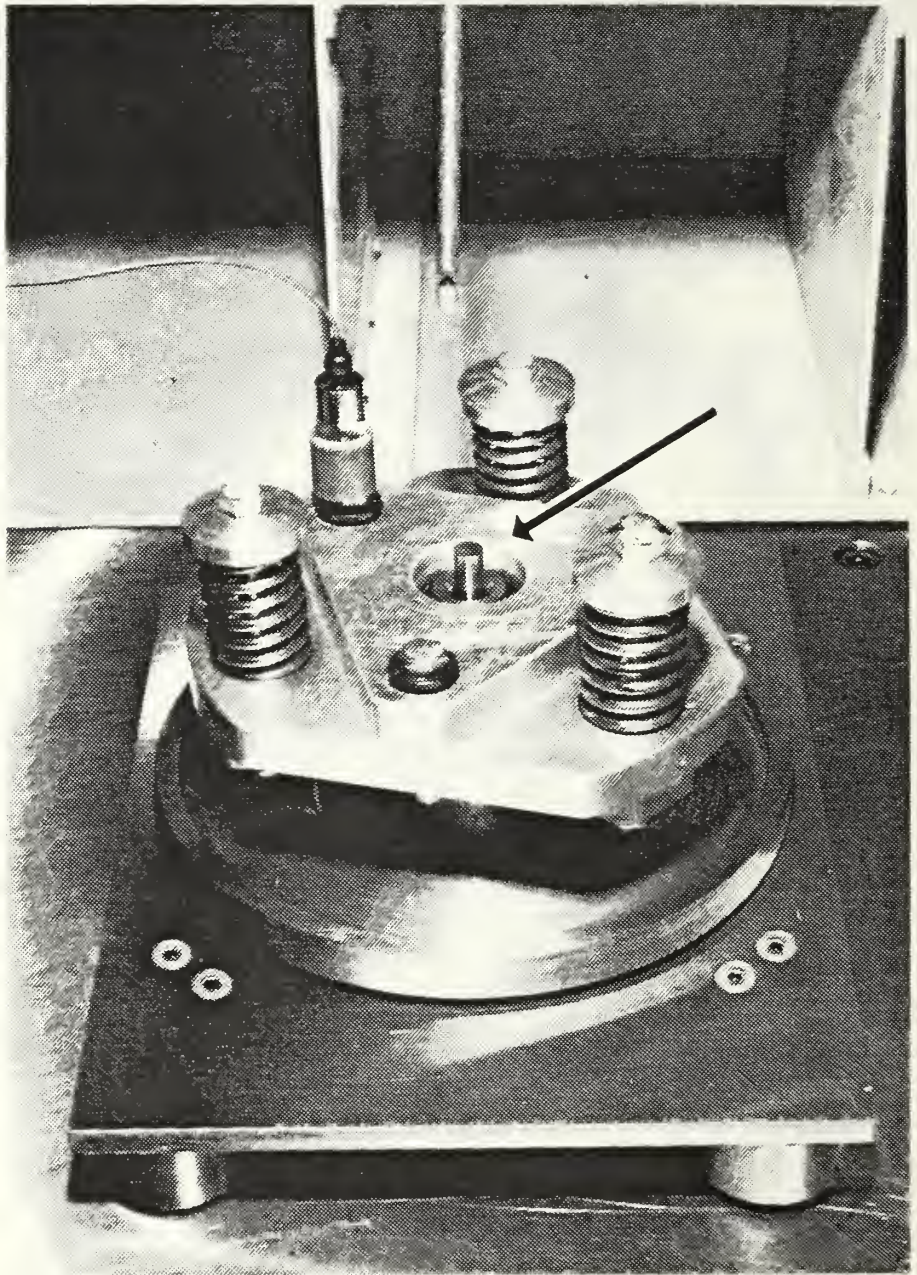


Figure 2.3. Ball-Rod Tester Used by Wright Aeronautical Laboratory. RCF Rod is Shown (Arrow) Mounted in Machine.

specimens used for microscopic examination were mechanically polished with diamond paste and etched with a mixture of 10 ml HCl, 3 ml HNO<sub>3</sub> and 100 ml ethyl alcohol.

Measurements of the maximum void dimension were taken directly from the SEM screen. The search for individual voids within a sample was conducted by randomly scanning across the specimen surface until at least 100 voids had been intersected and their maximum dimension recorded. The use of a maximum dimension corresponds to the diameter used for size distribution of spheres as discussed by Underwood [Ref. 8: p. 109]. The assumption of a spherical shape for the observed voids is an obvious simplification as evidenced by SEM micrographs found later in this study. However, this simplification is adequate for the purposes of this study in that it readily allows a relative comparison of the void dimensions found within the two conditions of M-50 steel. The search for voids was conducted at a magnification between 4000X and 5000X. Actual dimensional measurements were taken at 10,000X.

A total of four specimens were prepared for void size distribution measurements. A specimen from the transverse and longitudinal direction of both the as-received and warm-rolled condition was used. These specimens used for void size measurements had not been subjected to the austenitizing scheme documented below.

The data represented in Figure 2.4 illustrate the recording of such void dimension data for the longitudinal direction of the as-received condition. This figure consists of two significant features. The first is a histogram representing the raw data as measured from the SEM screen. The maximum dimension of each void encountered is recorded by the 0.1  $\mu\text{m}$  range within which it falls. Thus the voids encountered in the as received specimen fell within a range of 0.1  $\mu\text{m}$  to 2.3  $\mu\text{m}$ . There were four in the 0.2  $\mu\text{m}$  category, fourteen in the 0.4  $\mu\text{m}$  category, and so on. A smoothed curve is drawn above the histogram. This curve is a representation of the grouped data. Grouping the data consisted of breaking the raw data down into eight equally wide categories. Once this was accomplished a third order parametric curve was fit to the mid-points of the grouped categories of data. It is this curve that is shown above the raw data histogram.



# VOID SIZE DISTRIBUTION

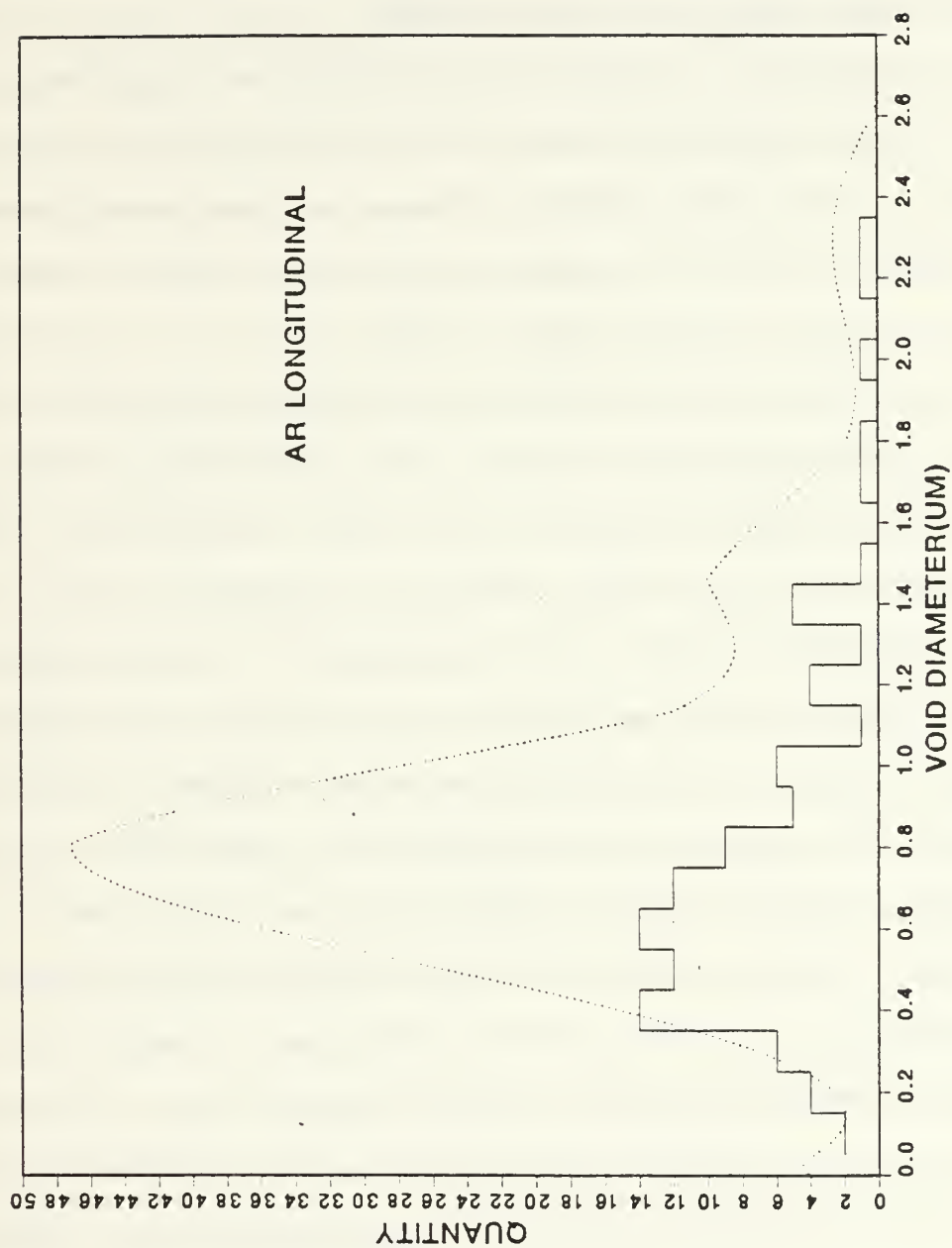


Figure 2.4. Void Size Distribution of As-Received Material in Longitudinal Direction. Histogram Represents Raw Data, Dotted Curve Represents Curve Fit Through Grouped Data.

### III. RESULTS AND DISCUSSION

#### A. ROLLING CONTACT FATIGUE TESTING

As discussed in the previous chapter on experimental procedures, RCF testing was carried out on either a disk-rod tester or a ball-rod tester. These two test apparatus are in widespread use in the bearing industry and are known to provide similar results for the same material. It should be emphasized that the RCF tests documented herein are relative rather than absolute in nature. The tests are relative in that the documented mean and  $L_{10}$  lives of a material under study are only valid when compared to the mean and  $L_{10}$  lives of a standard material. The standard for comparison is tested upon the same machine as the test material and in random sequence with the test material. This procedure insures that any bias associated with a particular testing machine is spread equally between the test and standard materials. Thus, results of RCF testing will be discussed by comparison of a test rod that has been machined from either as-received or warm-rolled material to a rod that is machined from standard M-50 material. The standard material is M-50 that has been forged and austenitized at  $1106^{\circ}\text{C}$  in keeping with standard industrial practice.

Documentation of RCF data is typically displayed in the form of a Weibull plot. This method of data display is

used in this study. The usefulness of the Weibull plot for reliability testing is well documented by Johnson [Ref. 9]. The methods of Johnson are widely used as a means of displaying RCF test data generated by bearing tests. Those methods of data analysis and data display are followed herein to display RCF data for as-received material (spheroidized anneal), warm-rolled material, and industry standard M-50 material (austenitized at 1106°C). Significant features of the Weibull plots are the logarithmic representation of sample lifetime along the plot abscissa, cumulative failure percentages along the ordinate,  $L_{10}$  life (i.e., that lifetime at which 10 percent of the test population will be expected to fail) and the least squares straight line fit to the individual RCF data points.

The first of five Weibull plots that follow is shown in Figure 3.1. The plot was developed from the data set of Appendix B denoted by the alphanumeric designation of F1. Each of the plots that follow were likewise developed from the appropriately labeled data set of Appendix B. Examination of Figure 3.1 shows that the RCF characteristics of specimen F1 (as-received material, austenitized at 1106°C) is quite similar to that of the M-50 standard to which it is compared. The Weibull slope of F1 is 2.02 while that of the standard is 1.74. The  $L_{10}$  life of F1 is  $15.35 \times 10^6$  cycles while that of the standard is a similar  $18.83 \times 10^6$  cycles.

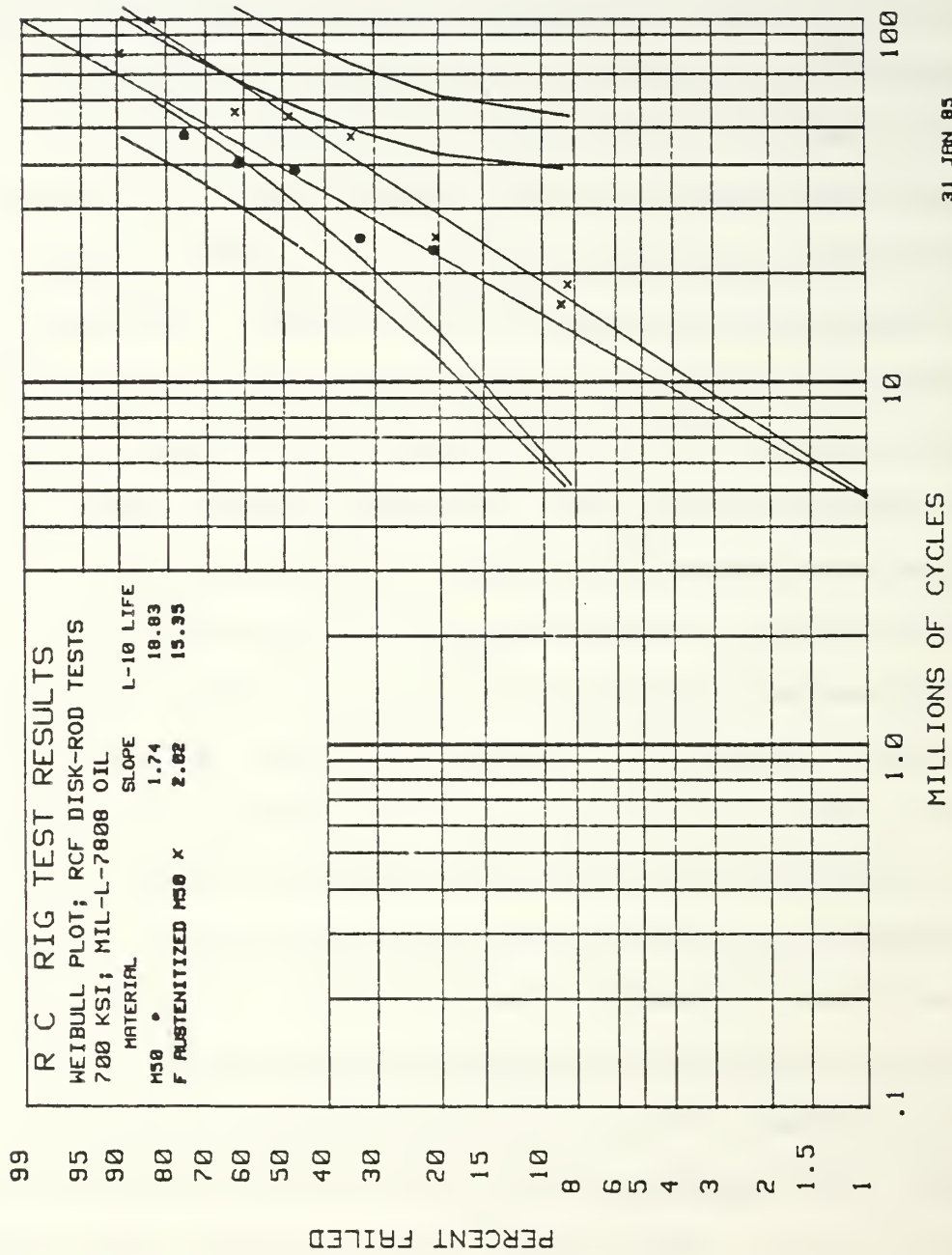


Figure 3.1. Weibull Plot for Specimen F1 (As-Received) Compared to Standard M-50 Material. F1 was Austenitized at 1106°C for 5 Minutes.

Furthermore, the plotted curve for F1 falls within the 90% confidence band of the standard and the plotted curve for the standard falls within the 90% confidence band of specimen F1. Within the scatter of the RCF data we can conclude that the materials behave in an essentially identical manner. This is not surprising in that both materials have been austenitized at the same temperature. This closeness in response to RCF testing is reassuring since the material heat treated in this study behaves in the same manner as the standard against which it is being compared. Knowing this, the remainder of the RCF test data can be viewed with a high degree of confidence.

The next three Weibull plots deal with warm-rolled material. The austenitizing temperature in all three cases was  $1036^{\circ}\text{C}$ . This temperature was chosen to produce the desired hardening with minimal grain growth and was based upon the previous work of Bres and of Butterfield. This choice has since been verified by Camerino [Ref. 10]. The work of Camerino has proceeded concurrently with this study, and has shown that an austenitizing temperature of  $1040^{\circ}\text{C}$  will produce a hardness in warm-rolled M-50 that is equivalent to the hardness attained in as-received material that is austenitized at  $1106^{\circ}\text{C}$ .

Figure 3.2 contrasts the RCF life data of specimen N to that of the standard. Specimen N has been warm-rolled at



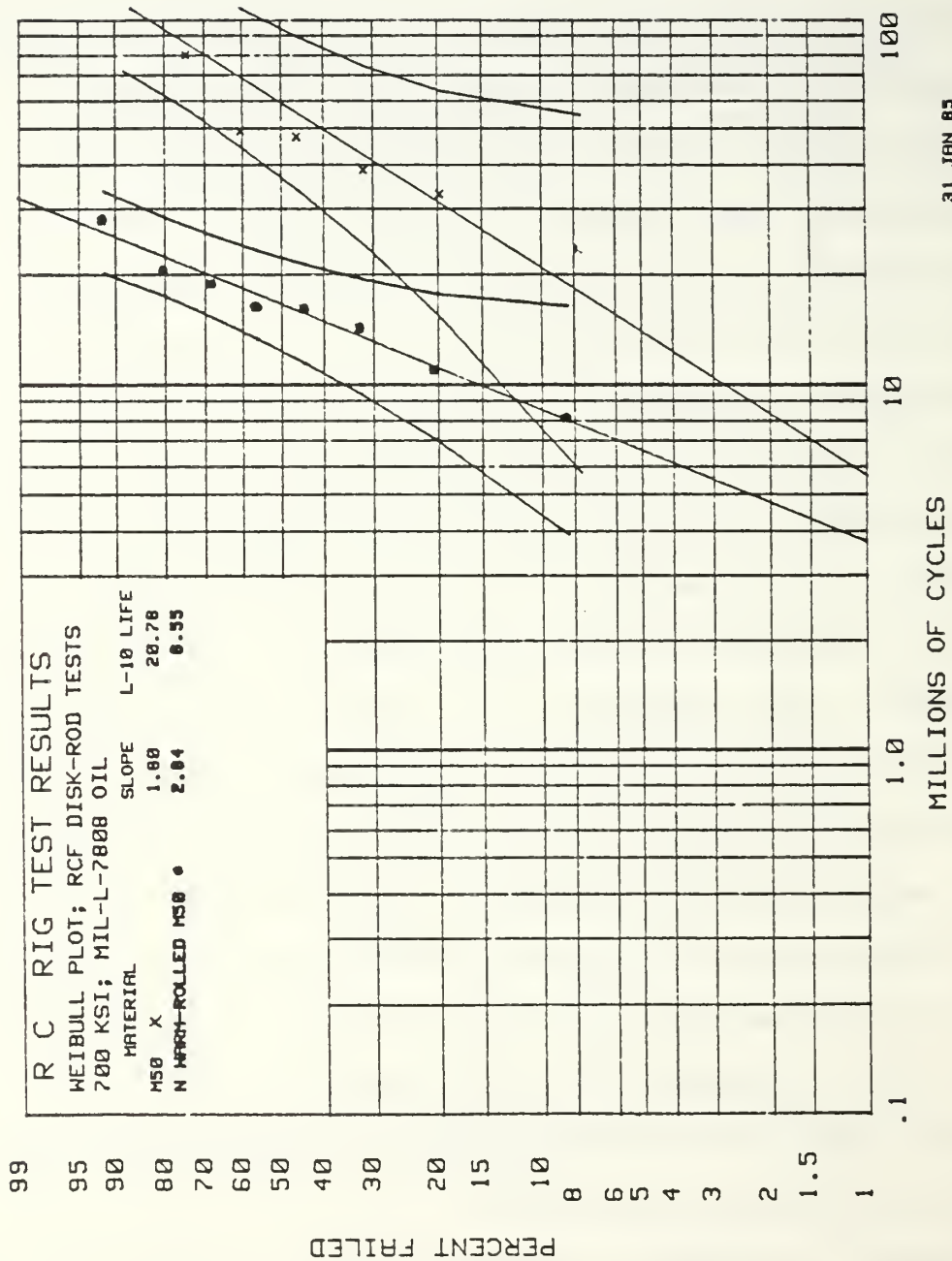


Figure 3.2. Weibull plot for Specimen N (Warm-Rolled) Compared to Standard M-50 Material. N was Austenitized at 1036°C for 5 Minutes.

750°C and austenitized at 1036°C for five minutes. From this plot it is apparent that the warm-rolled material is inferior to the standard material at all levels of failure. The  $L_{10}$  life of the warm-rolled material is  $8.55 \times 10^6$  cycles while that of the standard is  $20.78 \times 10^6$ . At higher failure percentages the spread between the lives of the materials continues to widen. From this it must be concluded that the warm-rolled material is inferior to the standard.

Figure 3.3 represents the plot of the RCF data for specimen D as compared to the standard material. Specimen D has been warm-rolled at 750°C and austenitized at 1036°C for a one minute period. Examination of the plot again reveals an inferiority of warm-rolled material. In this instance the warm-rolled material had been austenitized for a much shorter period than specimen N. However, this difference has had little if any effect upon the RCF life of the warm-rolled specimen. Again the  $L_{10}$  life of the warm-rolled material is substantially less than that of the standard material,  $6.21 \times 10^6$  cycles versus  $17.15 \times 10^6$  cycles. Note also that the disparity between lives again increases as the probability of failure increases.

Figure 3.4 represents the RCF data for specimen F2. This specimen was warm-rolled at 750°C and austenitized at 1036°C for two minutes. As was the case with specimens N

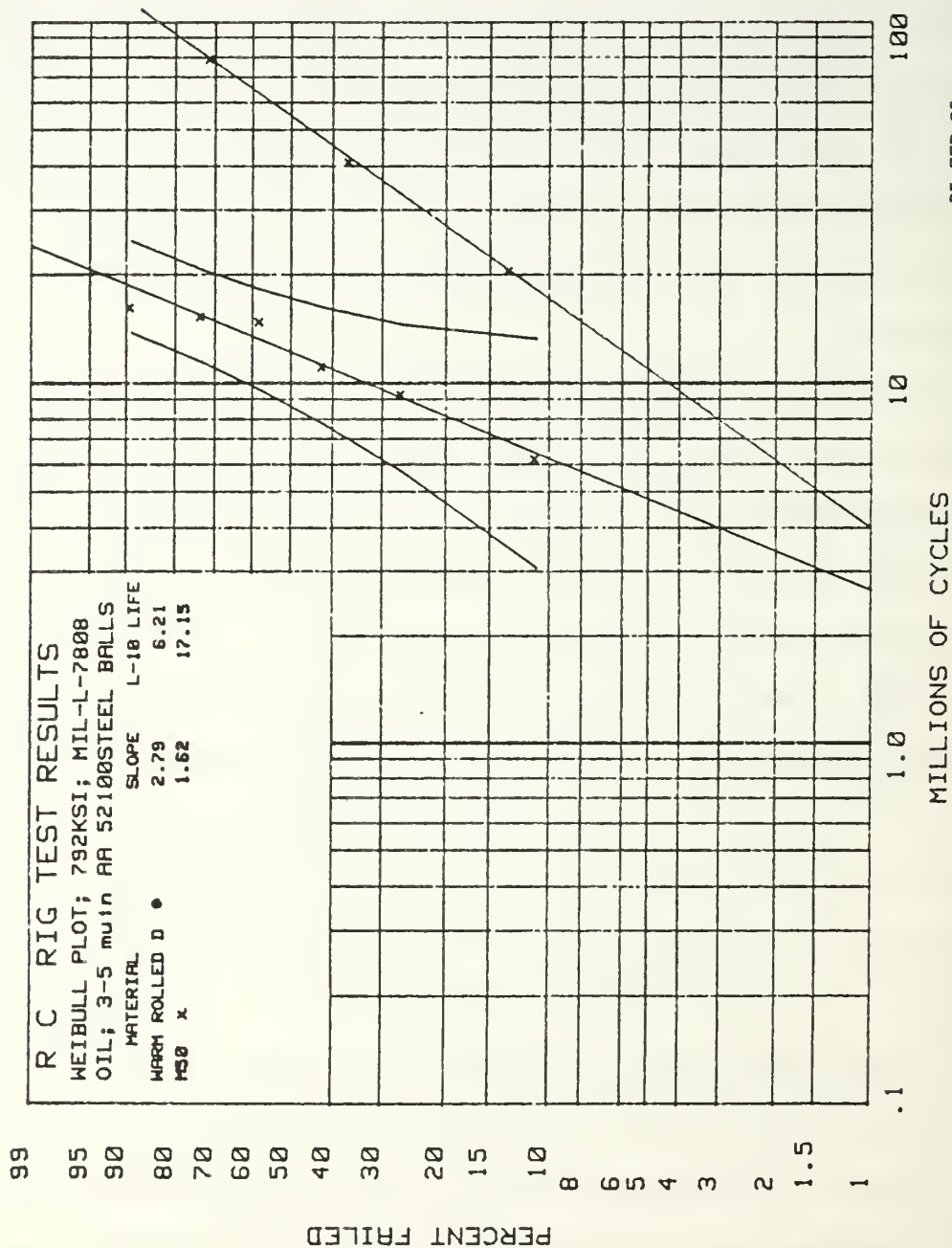


Figure 3.3. Weibull Plot for Specimen D (Warm-Rolled) Compared to Standard M-50 Material. D was Austenitized at 1036°C for 1 Minute.

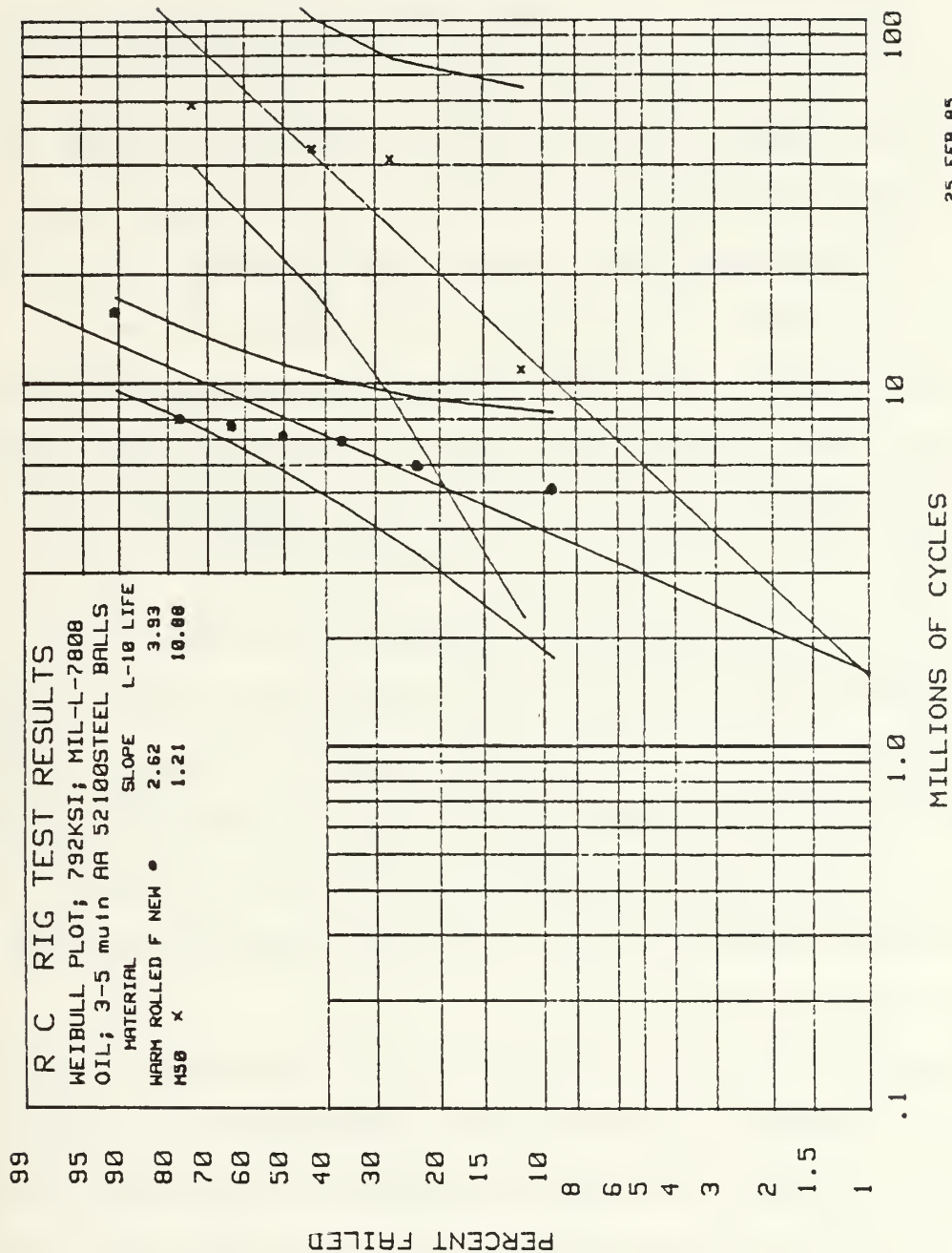


Figure 3.4. Weibull plot for Specimen F2 (Warm-Rolled) Compared to Standard M-50 Material. F2 was Austenitized at 1036°C for 2 Minutes.

and D the warm-rolled material is once again inferior to the standard material. The  $L_{10}$  life of the specimen F2 less than the  $L_{10}$  life of the standard,  $3.93 \times 10^6$  cycles versus  $10.88 \times 10^6$  cycles. Once again the Weibull slopes of the two plots are such that the disparity between lives of the warm-rolled material and the standard material widens as the probability of failure increases.

The last Weibull plot, Figure 3.5 presents RCF data from tests of specimen G. Specimen G was tested in the as-received condition following austenitizing at  $1036^{\circ}\text{C}$  for two minutes. This specimen was used to compare the RCF life of a specimen which had been underhardened to the standard material. By using the underhardened material a range of data can be established for comparison purposes. Not surprisingly, the RCF life of specimen G was substantially inferior to the RCF life of the standard material. Notable is the similarity between the RCF life of the underhardened specimen G and the warm-rolled specimens N, D, and F2. The post-temper hardness values of the RCF rods was measured and is given in Table 3.1.

Significantly, the hardness values obtained are in the range of Rockwell C 58 to 60. By comparison, the accepted standard hardness for bearing materials is about  $R_C 62$  [Ref. 11]. When the hardness readings for the tested RCF rods are compared to the results of the RCF tests there is no



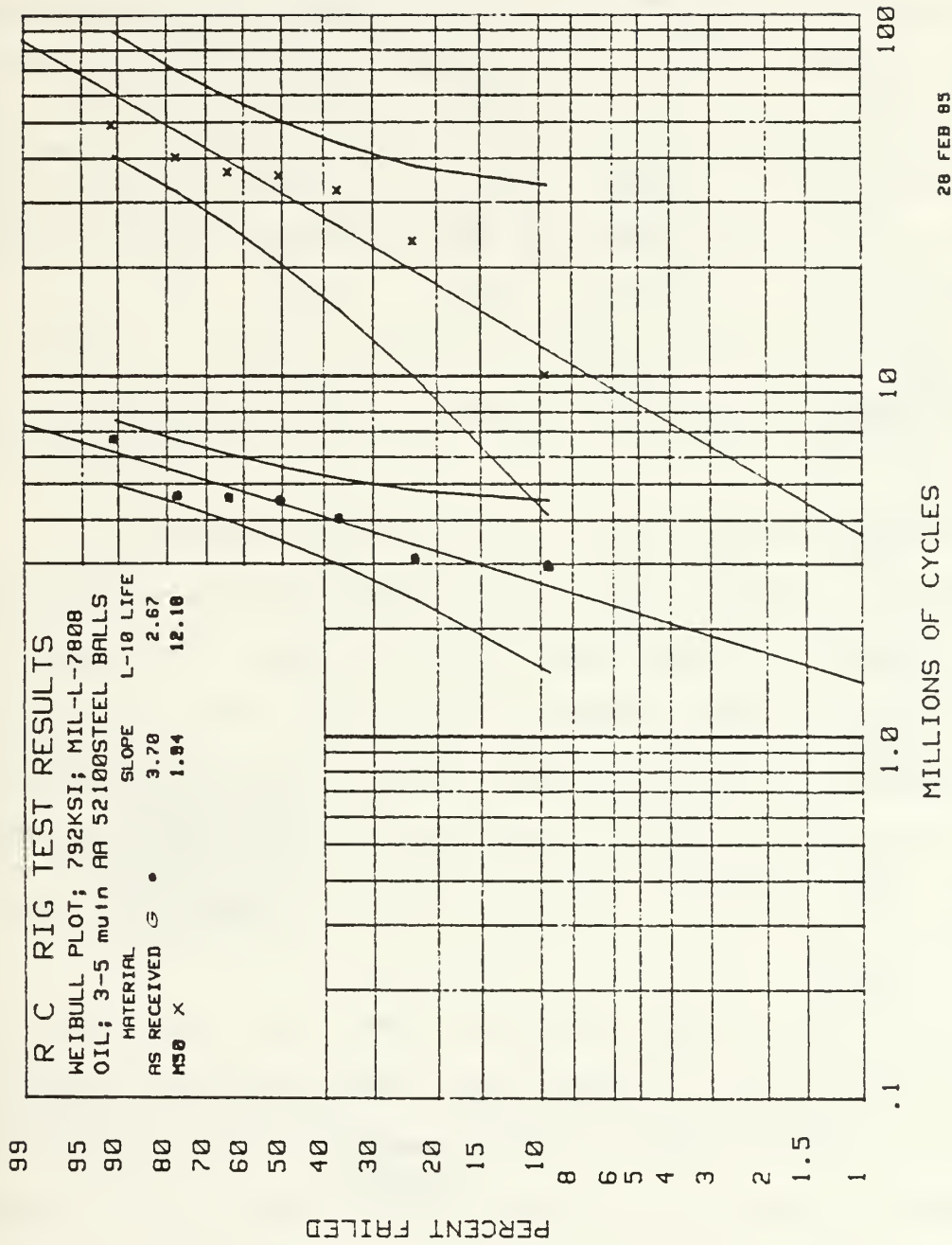


Figure 3.5. Weibull Plot for Specimen G (As-Received) Compared to Standard M-50 Material. G was Austenitized at 1036°C for 2 Minutes.

TABLE 3.1  
HARDNESS OF RCF RODS

Specimen	F1	N	F2	D	G
Condition	AR	WR	WR	WR	AR
Heat Treatment	1106°C 5 min	1036°C 5 min	1036°C 2 min	1036°C 1 min	1036°C 2 min
Hardness $R_c$	59.4	58.8	60.3	59.1	58.3
Standard Deviation	0.49	0.51	0.78	0.13	0.78

correlation between RCF life and material hardness evidenced. Tallian [Ref. 12] reported similar experiences for material hardness range of  $R_c 56$  to  $R_c 64$ . This lack of correlation between hardness and RCF life thus eliminates hardness as a factor that might account for the disparity in RCF test results that are documented above. The fact that others have reached a similar conclusion lends credence to this finding.

Following a suggestion by Wu [Ref. 13], results of the five Weibull plots obtained from testing the five RCF rod conditions were summarized for comparison of a single graph as shown in Figure 3.6. The graph is a plot of life ratio versus reliability percentage. Reliability percentage is obtained by subtracting failure percentage from 100 ( $R=1-F$ )

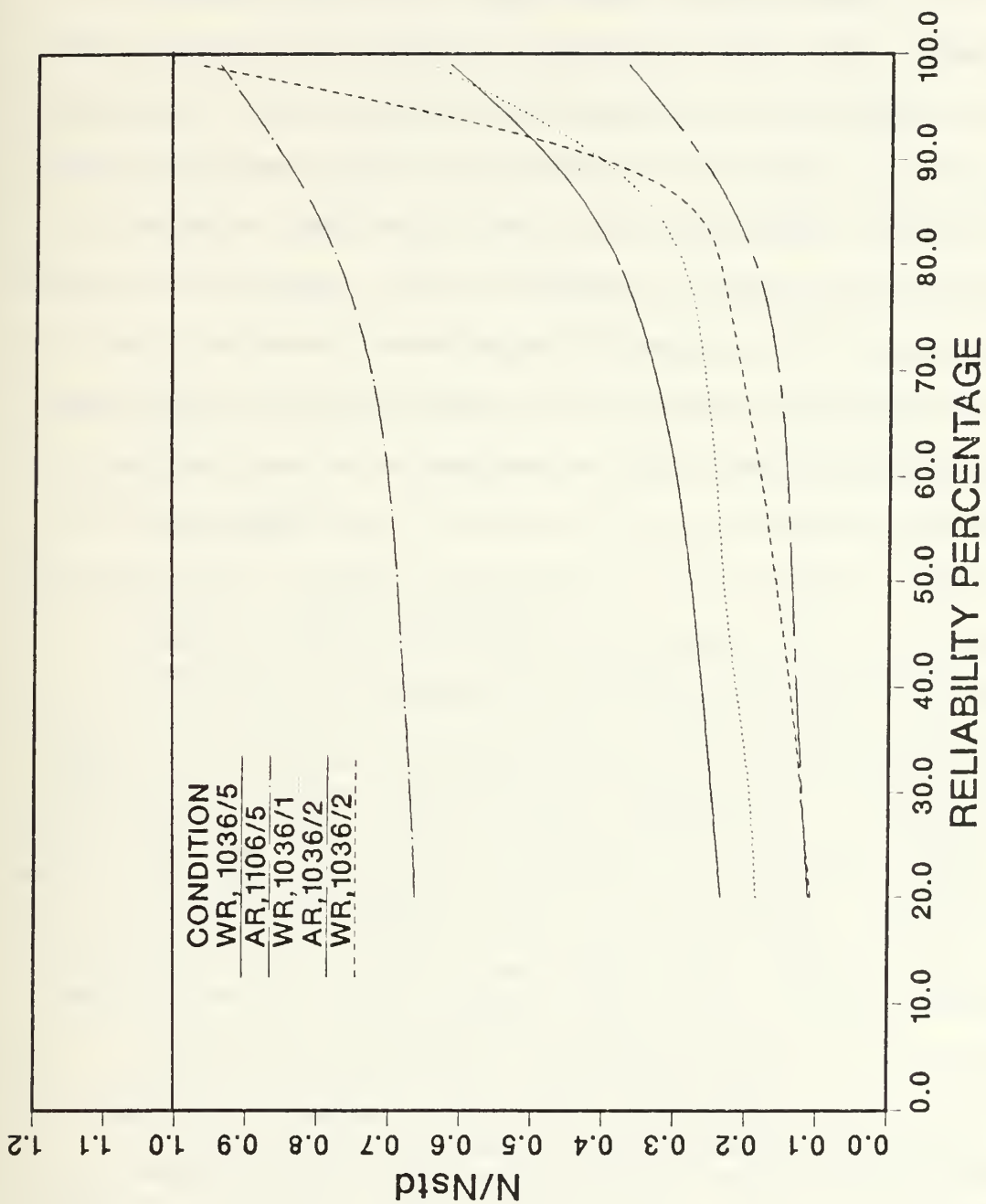


Figure 3.6. RCF Life Summary. Warm Rolling is Believed to Have Increased Void Dimensions Causing RCF to be Degraded.

and the life ratio is obtained by dividing the life of the condition of interest at a particular failure percentage by the life of the standard material at the same failure percentage. The above procedure was applied to each of the RCF rods tested and a curve smoothed through the calculated data points. Note the horizontal line that spans the width of the graph. This represents the curve that would be obtained if the material condition being tested were to give the identical RCF results of the standard material. As such, any material condition that gave data that fell above this horizontal line would be considered to be superior to the standard material at all levels of reliability percentage. Similarly, any material condition that produces a curve that falls below the horizontal line must be considered to be inferior to the standard material.

As noted earlier in this discussion, specimen F1 comes quite close to representing the same RCF characteristics of the standard material. It is not surprising then to see the curve for specimen F1 on Figure 3.6 falls closer to the horizontal than do the curves representing the warm-rolled specimens or the underhardened, as-received material, specimen G. The curves of Figure 3.6 descend from the horizontal as the mean life of the RCF rods decreases.

From the foregoing, all warm-rolled specimens fell short of reaching the RCF response of the material austenitized in

accordance with industry standards, i.e., 1106°C. The fact that warm rolling causes an obvious degradation of RCF life of M-50 steel, on both a mean life and  $L_{10}$  basis, immediately raises the question of why has this occurred. As noted in the introductory chapter of this study, Butterfield reported the existence of porosity associated with residual carbides in both the as-received and warm-rolled conditions. In the following, results of efforts to more thoroughly document this observation are reported. Such porosity may be important in crack initiation and consequently may be an important factor in the RCF lives of these materials.

#### B. POROSITY CHARACTERIZATION

Voids were found to exist in both the as-received and warm-rolled conditions of M-50. It is surprising to find voids within the as-received microstructure. The origin of them, and the likelihood of finding them in other heats of M-50 will be considered later in this section. With these observations in mind an attempt has been made to gain some insight into the character of the porosity and to statistically quantify the void dimensions.

To do this four specimens were prepared for scanning electron microscopy (SEM) examination. The specimens were prepared from only the warm-rolled and as-received conditions prior to any hardening treatment. This was done



to prevent any heat treating effects from obscuring the effects of warm rolling on void dimensions. Since the rolling used in this study resulted in a bar product, individual specimens were examined from the transverse and longitudinal directions only.

Results of the void measurements are summarized in Appendix C. The graphs contained in the appendix represent the accumulated data for each examined direction of the two conditions, warm-rolled and as-received. It is significant that the smoothed curve has the characteristic skewed tail expected for a log-normal distribution. Rhines [Ref. 14] relates this distribution form to many typically small particle size distributions. Working with the assumption that the grouped data is indeed distributed in a log-normal fashion, the grouped data was transformed to the natural log of the void diameters and plotted against quantity of voids within the group. Data in this form is displayed in both Figures 3.7 and Figure 3.8. When displayed in this form the data indeed closely approximate a normal distribution shape, hence the assumption of a log-normal distribution is validated.

For comparison purposes, the data for the transverse direction of both the as-received and the warm-rolled condition is displayed together. This side by side display of data allows the rightward shift of the warm-rolled curve to

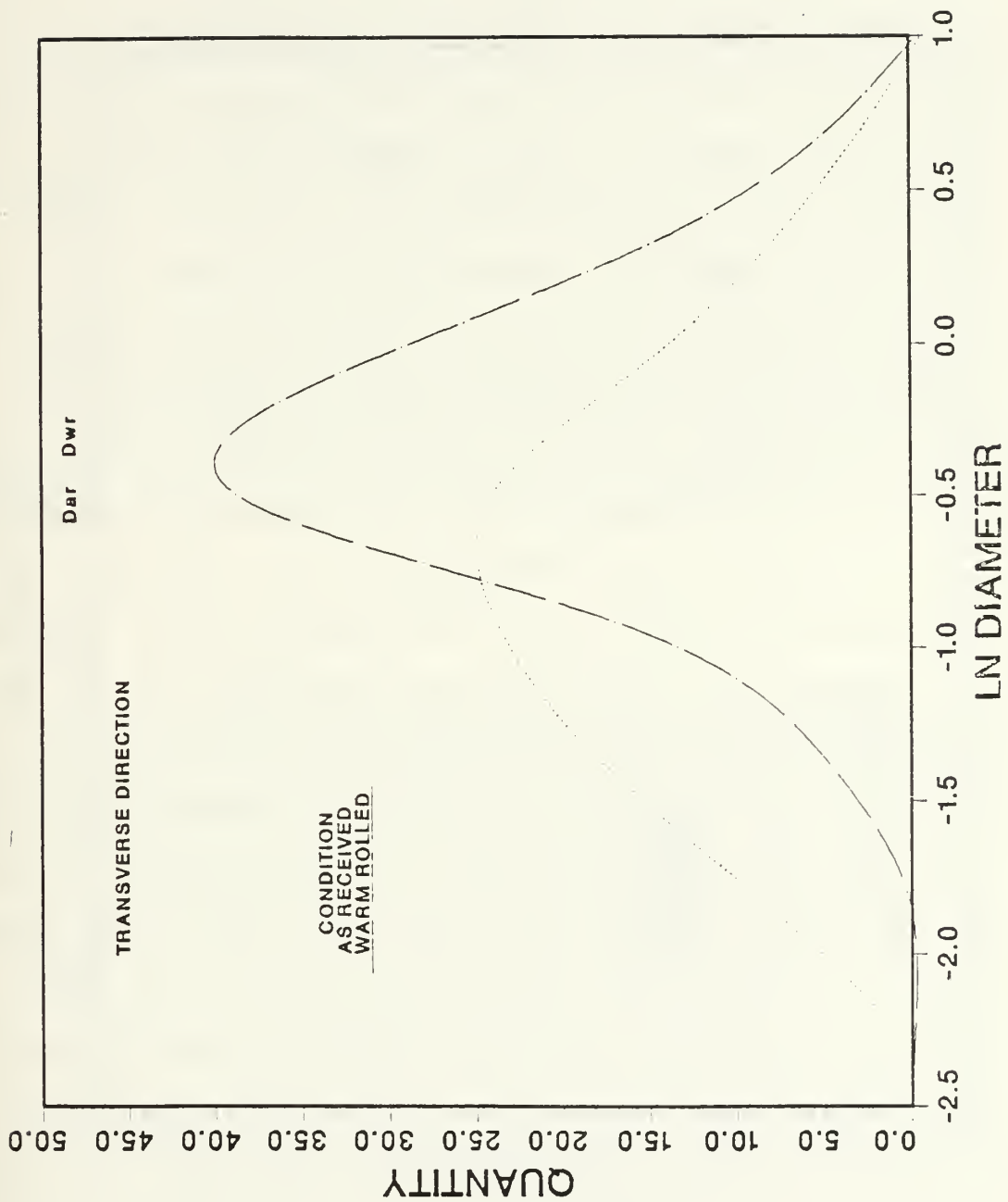


Figure 3.7. Comparison of Void Size Distributions, Transverse Direction

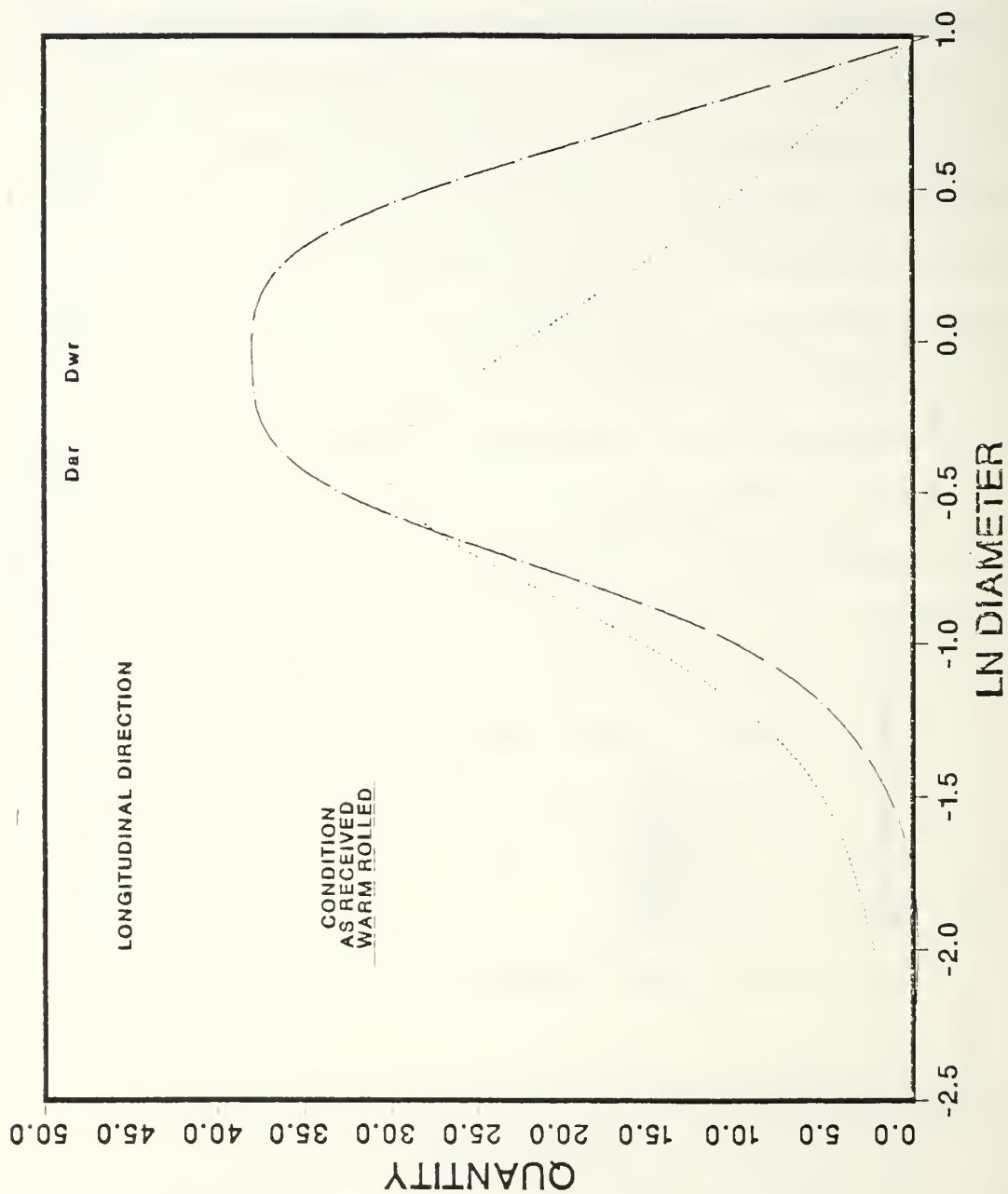
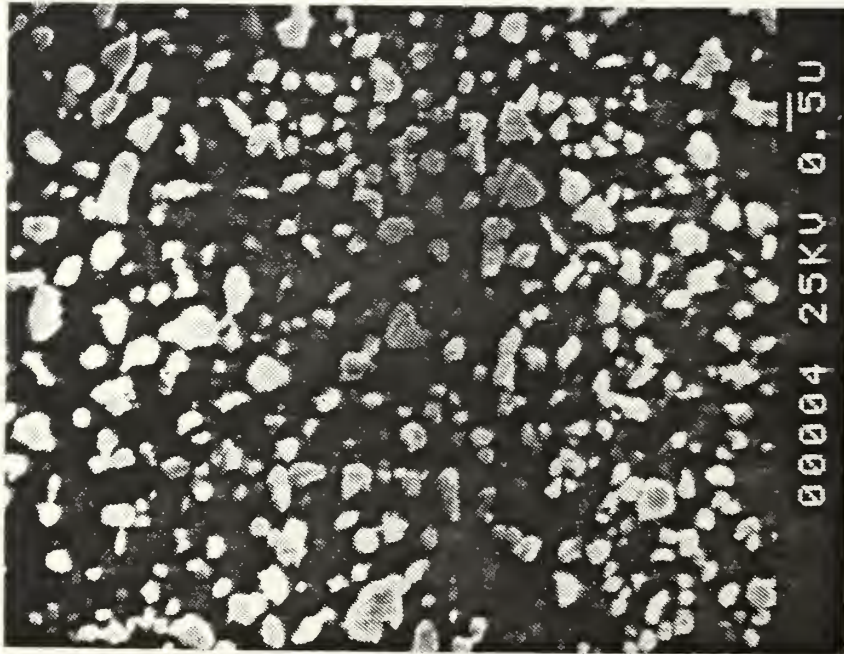


Figure 3.8. Comparison of Void Size Distribution, Longitudinal Direction

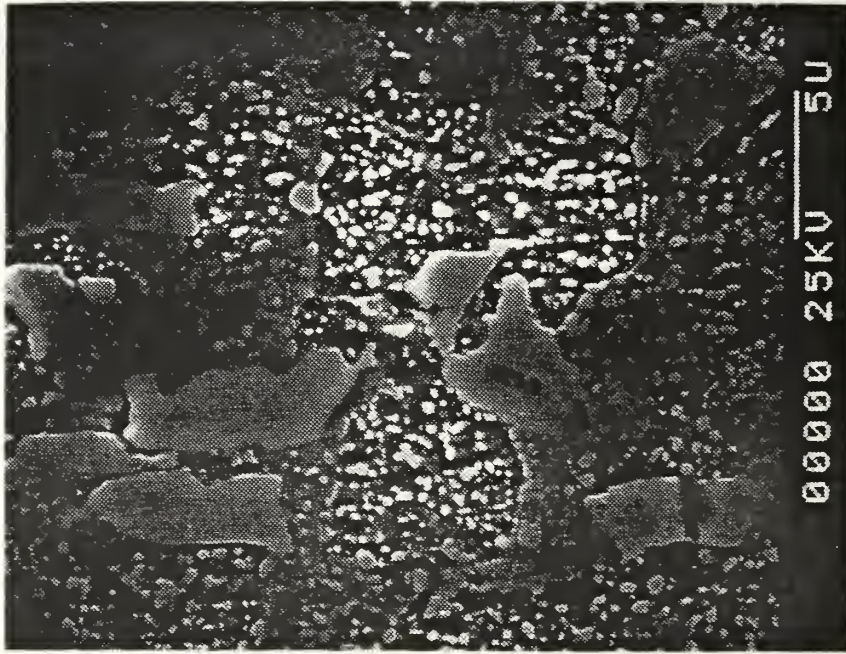
become apparent. Since the void size distribution is of a log-normal form, the geometric mean has been calculated for each of the two conditions. These values appear near the top of the graph.  $D_{ar}$  represents the geometric mean of the as-received material while  $D_{wr}$  represents the geometric mean of the warm-rolled material. The calculated value of  $D_{ar}$  is 0.485  $\mu\text{m}$ , while the calculated value of  $D_{wr}$  is 0.768  $\mu\text{m}$ .

As was done for the transverse direction, the data for the longitudinal direction of both the as-received and warm-rolled conditions is simultaneously displayed in Figure 3.8. Once again a rightward shift of the size distribution curves from the as-received condition to the warm-rolled condition is discernable. In this case the geometric mean of the as-received condition,  $D_{ar}$ , is 0.629  $\mu\text{m}$ , while the geometric mean of the warm-rolled condition,  $D_{wr}$ , is 0.882  $\mu\text{m}$ .

As is shown in the accompanying SEM micrographs, voids are quite evident in both the as-received material and the warm-rolled material. Furthermore the voids are easily identified in both the transverse and longitudinal directions of both material conditions. Figure 3.9 compares the microstructural features of the transverse and longitudinal directions of the as-received specimen. The voids in evidence are typically associated with a residual carbide. The void dimensions may be derived by comparison with the scale bar shown at the bottom of each micrograph. Figure 3.10



A



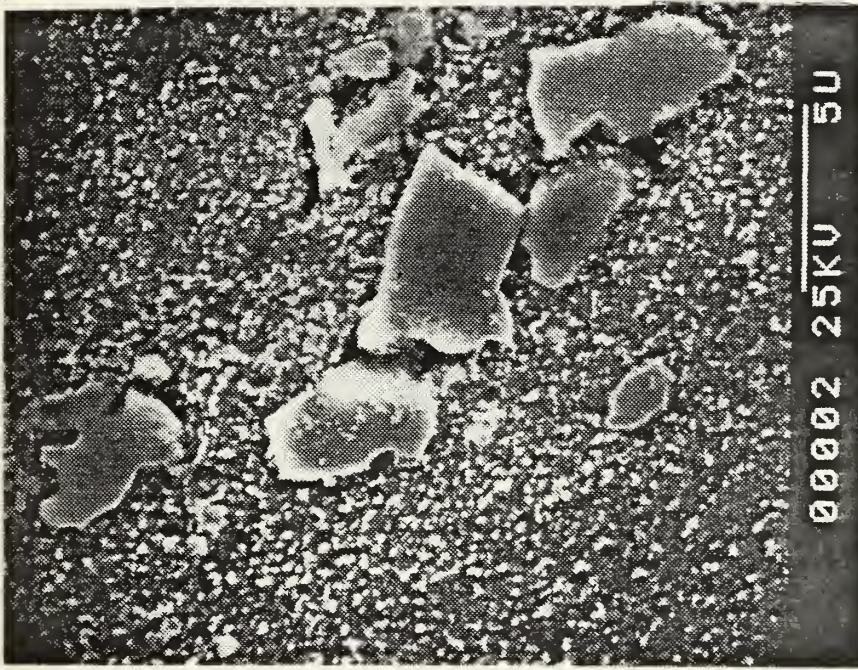
B

Figure 3.9. SEM Micrographs, As-Received Material. A is from the Transverse Direction, B is from the Longitudinal Direction.





A



B

Figure 3.10. SEM Micrographs, Warm-Rolled Material. A is from the Transverse Direction, B is from the Longitudinal Direction.

similarly presents the longitudinal and transverse views of the warm-rolled material. As was the case with the as-received material, those voids in evidence are associated with large massive residual carbides. These large carbides have been identified by Bridge, et. al. [Ref. 15] to be MC and  $M_2C$ . Vincent, et. al. [Ref. 16] reported diameters of MC ranging up to 30  $\mu m$ . The massive carbides viewed in this study were typically 5 to 10  $\mu m$  in diameter. It is these residual carbides to which the wear resistance of M-50 steel is attributed.

Given that voids were present in the as-received material, the increase in void diameter with warm-rolling is reasonable. The increase in void size is of particular interest since the stress intensity associated with the larger voids can be expected to increase in proportion to (void diameter)<sup>1/2</sup>. Also, it is noteworthy that the number of larger voids increases with warm-rolling. Thus, there are more large voids available to act as initiators for the most severe cracks.

### C. VOID FORMATION

Following the above data gathering, a bearing that had been taken out of service was sectioned for SEM examination. The bearing was obtained from the Naval Air Rework Facility and was fabricated from M-50 steel. Micrographs of this bearing are shown in Figure 3.11. As in the case of





Figure 3.11. SEM Micrographs, Bearing Race

as-received M-50 material, voids in the vicinity of residual carbides are in evidence. No attempt was made to quantify the void dimensions found in this bearing. However, the presence of voids in the fabricated bearing extends the finding of porosity in M-50 steel beyond the heat from which the material of this study was taken.

Given the evidence of voids within the M-50 micro-structure, the question of their origin immediately comes to mind. Figure 3.12 represents a schematic of a conceptual model that may account for the origin of voids and their diametral increase with warm rolling. Initially, M-50 is represented by the block of Step 1. This block of material is made up of a deformable matrix surrounding a hard spherical carbide. Step 2 pictures the space which the carbide occupies within the matrix. The space is obviously of the same shape and size as the carbide which occupies the space. This is analogous to a residual carbide resting within the cast M-50 matrix. Step 3 represents the deformation of the original block of material. In this case the matrix is elongated as could be expected to happen in the early stages of mechanically processing a cast material. At this point the space occupied by the carbide tends to deform with the matrix. However, the carbide is assumed not so readily deformed and thus tends to retain its original shape. This mismatch in ability to deform would



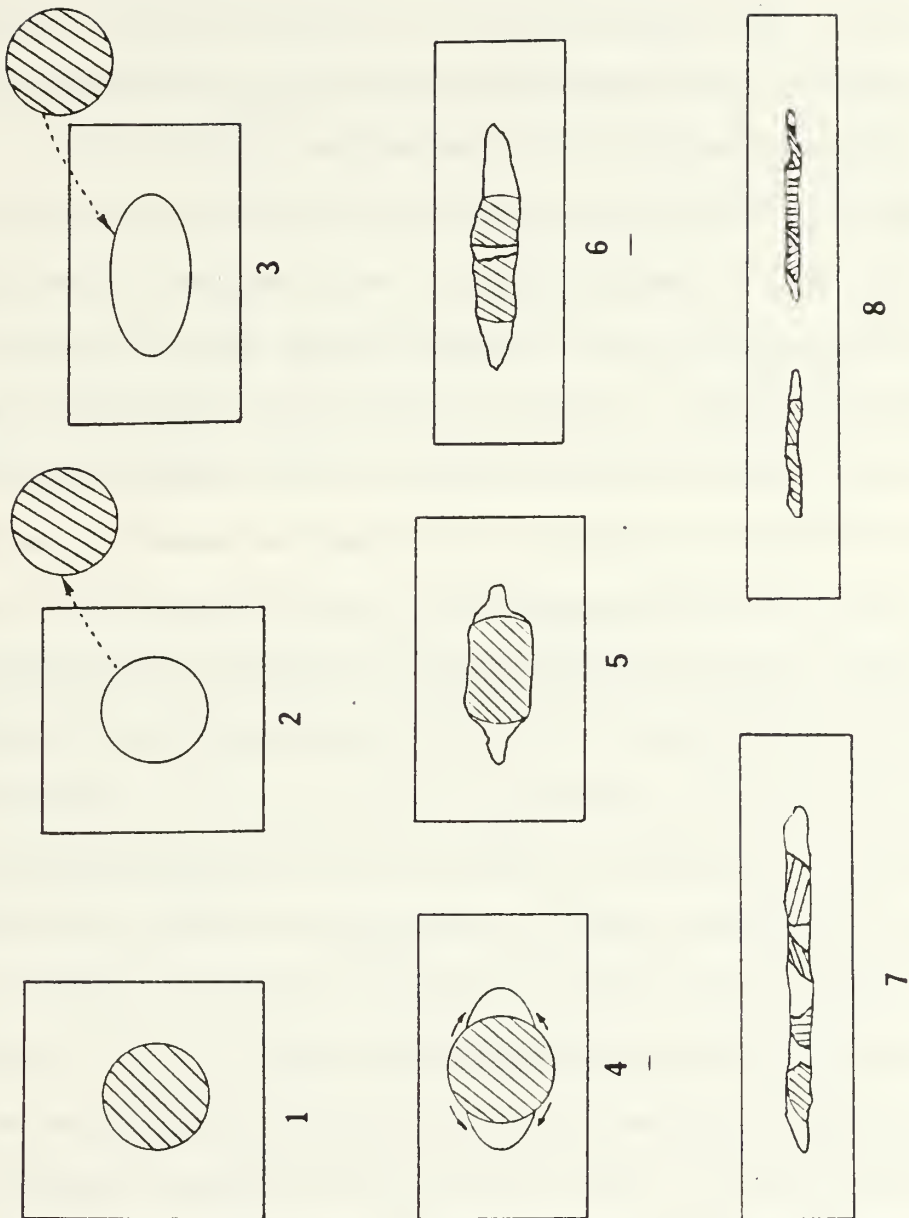


Figure 3.12. Conceptual Model for Void Formation



lead to Step 4. Here the nondeforming carbide is resting within the deformed matrix. The matrix attempts to accommodate the situation by flowing around the carbide to fill in the space on either side of the carbide. It is at this point that debonding at the carbide-matrix interface could occur. Such debonding would allow the matrix to pull away from the carbide and assume the configuration represented in Step 5. As-received material apparently reflects such a configuration. As previously noted the as-received microstructure contains voids in the vicinity of residual carbides. Step 6 of the model represents the beginning of warm rolling. During warm rolling the matrix would be further deformed by successive passes through a bar mill. As the cross section of the M-50 matrix is reduced by warm rolling it is likely that fracturing of the residual carbides would occur. Once fractured the carbide pieces would be carried further apart as the matrix continues to elongate as in Step 7. Finally, the carbide pieces would be strewn through the matrix with voids intermingled among them. Step 8 is representative of the warm-rolled microstructures examined in this study.

The steps proposed by this model are supported by features observed within the microstructures of M-50 specimens. As previously shown in Figure 3.9, voids are present within the as-received material. These features

correspond to Step 5 of the model. Figure 3.13 shows two examples of fractured carbides that correspond to Step 6. Finally, Figure 3.14 shows two examples of warm-rolled microstructures that support Step 7 and Step 8 of the Model.

The proposed association between residual carbides and voids in the M-50 microstructure was reinforced after examination of over four hundred voids within the specimens examined with the SEM. One interesting feature that is not completely evidenced by the enclosed micrographs is the regions in which no voids or carbides were found. While scanning a specimen surface it was usual to find that relatively large areas were free of residual carbides and consequently free of voids. This observation was not surprising since the banding of residual carbides within the various tool steels is well known and recognized as being a problem area.

It has been suggested that carbides may have a concentrating effect on stresses in tool steels [Ref. 17]. Furthermore, it is widely believed that failures begin as subsurface cracks in bearing materials and that such cracks begin at the point of maximum Hertzian stress in the case of RCF failures.

An additional aspect of this problem now brought out in this research is the possible presence of a population of



Figure 3.13. Fractured Carbides Within As-Received M-50



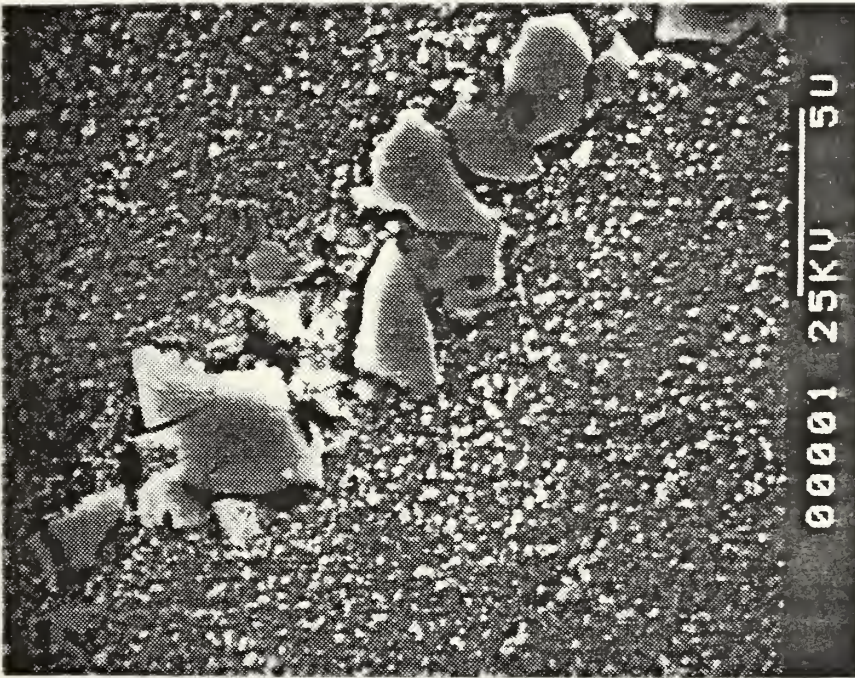


Figure 3.14. Carbide Pieces Strewn Through Warm-Rolled Microstructures

voids in association with these carbides. These fine voids would be difficult to detect given their generally small size and association with the massive carbides. Recall that magnifications of 5000X were required to reveal these voids. The very association with the massive carbides suggests their probable importance in the processes involved in cracking and spall formations. With such voids present in regions of high contact stress, crack initiation would be facilitated either in the matrix or the carbide. Here, the warm rolling has refined the matrix but increased the severity of the voids and, as such, the predominant effect of this appears to be the decrease in fatigue resistance noted. Any benefit of matrix refinement has been overshadowed by the enhanced void size.

This naturally suggests that means be sought to remove or reduce the porosity by hot isostatic pressing (HIP) and then evaluate the RCF behavior. Removal of such voids would test the hypothesis that they degrade fatigue resistance. This should first be evaluated for as-received material. If fatigue life is enhanced by HIP, further attempts to close voids in the rolled material should follow. This would facilitate direct comparison of the matrix structures.



#### IV. CONCLUSIONS AND RECOMMENDATIONS

##### A. CONCLUSIONS

- 1) Warm rolling of AISI M-50 steel degrades the RCF life of the material at both the  $L_{10}$  and  $L_{50}$  levels.
- 2) Warm rolling of M-50 steel increases the mean void diameter of those voids that are present in the as-received material.
- 3) Voids in M-50 steel are present in quantity and are typically found adjacent to residual carbides within the steel microstructure.
- 4) Warm-rolled RCF test rods produce less scatter in the failure data than do standard material test rods. This is reflected in the steeper Weibull slope of the warm-rolled data. This fact suggests that warm rolling is producing a more uniform structure within the material.
- 5) The process of void formation and enlargement is apparently a result of mechanical processing of the material and is due to the inability of residual carbides to deform in the same manner as the matrix in which they rest.

##### B. RECOMMENDATIONS

- 1) The possibility that hot isostatic pressing (HIP) may partially or completely close the voids within the as-received M-50 microstructure should be investigated. It is reasonable to expect that a reduction in the mean void diameter and a reduction in the quantity of larger void diameters would increase the RCF of M-50 steel. HIPing may be able to accomplish this.
- 2) Conduct RCF testing of warm-rolled M-50 that had been austenitized at  $1106^{\circ}\text{C}$  ( $2023^{\circ}\text{F}$ ). The data of this study suggest a slight correlation between austenitizing temperature and RCF life as well as between time spent at austenitizing temperature and RCF life.

Austenitizing at 1106°C would help discern any relationship between austenitization of warm-rolled M-50 at the industry standard temperature and RCF life.

# APPENDIX A

Material Condition	Austenitizing Schedule	
	<u>Butterfield</u>	<u>Perry</u>
As-Received	1006°C - 5 min	1036°C - 2 min
	1106°C - 5 min	1106°C - 5 min
Warm Rolled	1006°C - 5 min	1036°C - 1 min
	1036°C - 5 min	1036°C - 2 min
		1036°C - 5 min

# APPENDIX B

## TABLE I

### WEIBULL ANALYSIS OF ROLLING CONTACT FATIGUE TESTS:

#### WEIBULL PLOT: RCF DISK-ROD TESTS

TEST RIG / HEAD ===== 2  
 TYPES OF MATERIAL ===== F AUSTENITIZED M50  
 PIN NUMBER ===== F1  
 DISK OR BALL LOT NUMBER ===== 91-181  
 TEST OIL ===== 0-79-16H  
 DATE ===== 31 JAN 85  
 NUMBER OF TESTS ===== 9  
 TOTAL NUMBER OF FAILURES ===== 7

ORDER NUMBER	MEDIAN RANK	FAILED SPECIMEN	X VALUE	Y VALUE
1	.08596	16.50	+28.04E-01	-2.41E+00
2	.20425	23.36	+31.51E-01	-1.48E+00
3	.32255	25.12	+32.24E-01	-9.43E-01
5	.46451	38.86	+36.60E-01	-4.71E-01
6	.60647	40.82	+37.09E-01	+3.22E-01
7	.74843	48.16	+38.75E-01	+3.22E-01
9	.89039	81.04	+43.95E-01	+7.93E-01

### SPECIMEN LIFE VALUES WITH 90% CONFIDENCE BANDS:

		LOWER BAND	UPPER BAND
L(10) LIFE =	15.35	6.83	33.48
L(50) LIFE =	39.05	27.18	56.11

WEIBULL SLOPE = 2.0170  
 CORRELATION COEFFICIENT = .83214  
 CHARACTERISTIC LIFE = 47.01  
 MEAN LIFE = 41.49  
 F[X] = .54  
 X-MEAN = .354529E+01  
 STANDARD DEVIATION OF X = .529042E+00  
 STAN. DEV. OF X--SQUARED = .279886E+00

TABLE II

WEIBULL ANALYSIS OF ROLLING CONTACT FATIGUE TESTS:

## WEIBULL PLOT: RCF DISK-ROD TESTS

TEST RIG / HEAD ===== 2  
 TYPES OF MATERIAL ===== M50  
 PIN NUMBER ===== T2  
 DISK OR BALL LOT NUMBER ===== 91-181  
 TEST OIL ===== 0-79-16H  
 DATE ===== 31 JAN 85  
 NUMBER OF TESTS ===== 8  
 TOTAL NUMBER OF FAILURES ===== 6

ORDER NUMBER	MEDIAN RANK	FAILED SPECIMEN	X VALUE	Y VALUE
1	.08300	18.77	+29.32E-01	-2.45E+00
2	.20214	25.43	+32.36E-01	-1.49E+00
3	.34114	47.98	+38.71E-01	-8.74E-01
4	.48014	54.45	+39.97E-01	-4.24E-01
6	.61914	55.92	+40.24E-01	-3.53E-02
7	.82765	100.42	+46.09E-01	+5.64E-01

SPECIMEN LIFE VALUES WITH 90% CONFIDENCE BANDS:

		LOWER BAND	UPPER BAND
L(10) LIFE =	18.83	6.99	47.77
L(50) LIFE =	55.60	35.98	85.88

WEIBULL SLOPE	=	1.7403
CORRELATION COEFFICIENT	=	.81361
CHARACTERISTIC LIFE	=	68.94
MEAN LIFE	=	61.14
F[X]	=	.56
X-MEAN	=	.377827E+01
STANDARD DEVIATION OF X	=	.602870E+00
STAN. DEV. OF X--SQUARED	=	.363452E+00



TABLE III

WEIBULL ANALYSIS OF ROLLING CONTACT FATIGUE TESTS:

WEIBULL PLOT: RCF DISK-ROD TESTS

TEST RIG / HEAD ===== 1  
 TYPES OF MATERIAL ===== N WARM ROLLED  
 PIN NUMBER ===== N  
 DISK OR BALL LOT NUMBER ===== 810-172  
 TEST OIL ===== 0-79-16H  
 DATE ===== 31 JAN 85  
 NUMBER OF TESTS ===== 8  
 TOTAL NUMBER OF FAILURES ===== 8

ORDER NUMBER	MEDIAN RANK	FAILED SPECIMEN MCYCLES	X VALUE	Y VALUE
1	.08300	8.16	+21.00E-01	-2.45E+00
2	.20214	11.07	+24.05E-01	-1.49E+00
3	.32128	14.37	+26.65E-01	-9.48E-01
4	.44043	16.22	+27.86E-01	-5.44E-01
5	.55957	16.42	+27.99E-01	-1.98E-01
6	.67872	18.96	+29.43E-01	+1.27E-01
7	.79786	20.49	+30.20E-01	+4.69E-01

SPECIMEN LIFE VALUES WITH 90% CONFIDENCE BANDS:

		LOWER BAND	UPPER BAND
L(10) LIFE =	8.5	4.66	15.13
L(50) LIFE =	16.60	12.71	21.67

WEIBULL SLOPE = 2.8393  
 CORRELATION COEFFICIENT = .86389  
 CHARACTERISTIC LIFE = 18.94  
 MEAN LIFE = 16.83  
 F[X] = .51  
 X-MEAN = .275739E+01  
 STANDARD DEVIATION OF X = .380477E+00  
 STAN. DEV. OF X--SQUARED = .144763E+00

TABLE IV

WEIBULL ANALYSIS OF ROLLING CONTACT FATIGUE TESTS:

## WEIBULL PLOT: RCF DISK-ROD TESTS

TEST RIG / HEAD ===== 1  
 TYPES OF MATERIAL ===== M50  
 PIN NUMBER ===== T1  
 DISK OR BALL LOT NUMBER ===== 810-172  
 TEST OIL ===== 0-79-16H  
 DATE ===== 31 JAN 85  
 NUMBER OF TESTS ===== 10  
 TOTAL NUMBER OF FAILURES ===== 7

ORDER NUMBER	MEDIAN RANK	FAILED SPECIMEN MCYCLES	X VALUE	Y VALUE
1	.07659	23.71	+31.66E-01	-2.53E+00
2	.19567	33.41	+35.09E-01	-1.52E+00
4	.31476	39.00	+36.64E-01	-9.73E-01
5	.45766	48.11	+38.74E-01	-4.91E-01
7	.60056	49.95	+39.11E-01	-8.59E-02
8	.74346	80.74	+43.91E-01	+3.08E-01
10	.88636	141.17	+49.50E-01	+7.77E-01

SPECIMEN LIFE VALUES WITH 90% CONFIDENCE BANDS:

		LOWER BAND	UPPER BAND
L(10) LIFE =	20.78	8.78	48.55
L(50) LIFE =	59.04	39.90	87.40

WEIBULL SLOPE = 1.8043  
 CORRELATION COEFFICIENT = .80547  
 CHARACTERISTIC LIFE = 72.65  
 MEAN LIFE = 64.31  
 F[X] = .55  
 X-MEAN = .392345E+01  
 STANDARD DEVIATION OF X = .589972E+00  
 STAN. DEV. OF X--SQUARED = .348067E+00

TABLE V

WEIBULL ANALYSIS OF ROLLING CONTACT FATIGUE TESTS:

WEIBULL PLOT: 792KSI: MIL-L-7808

TEST RIG / HEAD ===== 3.3  
 TYPES OF MATERIAL ===== WARM ROLLED D  
 PIN NUMBER ===== D  
 DISK OR BALL LOT NUMBER ===== 501  
 TEST OIL ===== 0-79-16  
 DATE ===== 25 FEB 85  
 NUMBER OF TESTS ===== 6  
 TOTAL NUMBER OF FAILURES ===== 6

ORDER NUMBER	MEDIAN RANK	FAILED SPECIMEN	X VALUE	Y VALUE
1	.10910	6.24	+18.31E-01	-2.16E+00
2	.26546	9.39	+22.40E-01	-1.18E+00
3	.42182	11.20	+24.16E-01	-6.02E-01
4	.57818	14.91	+27.02E-01	-1.47E-01
5	.73454	15.43	+27.36E-01	+2.82E-01
6	.89090	16.31	+27.92E-01	+7.95E-01

SPECIMEN LIFE VALUES WITH 90% CONFIDENCE BANDS:

	LOWER BAND	UPPER BAND
L(10) LIFE = 6.21	3.03	11.54
L(50) LIFE = 12.19	9.07	16.37

WEIBULL SLOPE = 2.7906  
 CORRELATION COEFFICIENT = .81447  
 CHARACTERISTIC LIFE = 13.94  
 MEAN LIFE = 12.38  
 F[X] = .51  
 X-MEAN = .245278E+01  
 STANDARD DEVIATION OF X = .371715E+00  
 STAN. DEV. OF X--SQUARED = .138172E+00

TABLE VI

WEIBULL ANALYSIS OF ROLLING CONTACT FATIGUE TESTS:

WEIBULL PLOT: 792KSI: MIL-L-7808

TEST RIG / HEAD ===== 3.3  
 TYPES OF MATERIAL ===== M50  
 PIN NUMBER ===== 11  
 DISK OR BALL LOT NUMBER ===== 501  
 TEST OIL ===== 0-79-16  
 DATE ===== 25 FEB 85  
 NUMBER OF TESTS ===== 5  
 TOTAL NUMBER OF FAILURES ===== 3

ORDER NUMBER	MEDIAN RANK	FAILED SPECIMEN	X VALUE	Y VALUE
1	.12945	20.54	+30.22E-01	-1.98E+00
2	.36104	41.13	+37.17E-01	-8.03E-01
4	.70843	79.50	+43.76E-01	+2.09E-01

SPECIMEN LIFE VALUES WITH 90% CONFIDENCE BANDS:

		LOWER BAND	UPPER BAND
L(10) LIFE =	17.15	4.34	52.14
L(50) LIFE =	55.06	32.14	94.01

WEIBULL SLOPE = 1.6151  
 CORRELATION COEFFICIENT = .66642  
 CHARACTERISTIC LIFE = 69.42  
 MEAN LIFE = 61.89  
 F[X] = .57  
 X-MEAN = .370496E+01  
 STANDARD DEVIATION OF X = .676768E+00  
 STAN. DEV. OF X--SQUARED = .458015E+00

TABLE VII

WEIBULL ANALYSIS OF ROLLING CONTACT FATIGUE TESTS:

WEIBULL PLOT: 792KSI: MIL-L-7808

TEST RIG / HEAD ===== 3.2  
 TYPES OF MATERIAL ===== WARM ROLLED  
 PIN NUMBER ===== F2  
 DISK OR BALL LOT NUMBER ===== 501  
 TEST OIL ===== 0-79-16  
 DATE ===== 25 FEB 85  
 NUMBER OF TESTS ===== 7  
 TOTAL NUMBER OF FAILURES ===== 7

ORDER NUMBER	MEDIAN RANK	FAILED SPECIMEN	X VALUE	Y VALUE
1	.09428	5.16	+16.41E-01	-2.31E+00
2	.22952	5.99	+17.96E-01	-1.34E+00
3	.36476	7.02	+19.49E-01	-7.90E-01
4	.50000	7.22	+19.77E-01	-3.67E-01
5	.63524	7.69	+20.40E-01	+8.48E-03
6	.77048	8.05	+20.86E-01	+8.86E-01
7	.90572	15.79	+27.59E-01	+8.59E-01

SPECIMEN LIFE VALUES WITH 90% CONFIDENCE BANDS:

	LOWER BAND	UPPER BAND
L(10) LIFE = 3.93	1.94	7.44
L(50) LIFE = 8.08	5.97	10.91

WEIBULL SLOPE	=	2.6152
CORRELATION COEFFICIENT	=	.73585
CHARACTERISTIC LIFE	=	9.32
MEAN LIFE	=	8.25
F[X]	=	.52
X-MEAN	=	.203452E+01
STANDARD DEVIATION OF X	=	.354353E+00
STAN. DEV. OF X--SQUARED	=	.125566E+00



TABLE VIII

WEIBULL ANALYSIS OF ROLLING CONTACT FATIGUE TESTS:

WEIBULL PLOT: 792KSI: MIL-L-7808

TEST RIG / HEAD ===== 3.2  
 TYPES OF MATERIAL ===== M50  
 PIN NUMBER ===== 10  
 DISK OR BALL LOT NUMBER ===== 501  
 TEST OIL ===== 0-79-16  
 DATE ===== 25 FEB 85  
 NUMBER OF TESTS ===== 7  
 TOTAL NUMBER OF FAILURES ===== 4

ORDER NUMBER	MEDIAN RANK	FAILED SPECIMEN	X VALUE	Y VALUE
1	.11360	11.00	+23.98E-01	-2.12E+00
2	.26816	42.64	+37.29E-01	-1.16E+00
3	.42272	44.53	+37.96E-01	-5.99E-01
4	.73184	58.93	+40.76E-01	+2.75E-01

SPECIMEN LIFE VALUES WITH 90% CONFIDENCE BANDS:

		LOWER BAND	UPPER BAND
L(10) LIFE =	10.88	2.38	43.17
L(50) LIFE =	51.45	26.85	98.45

WEIBULL SLOPE = 1.2124  
 CORRELATION COEFFICIENT = .67985  
 CHARACTERISTIC LIFE = 70.07  
 MEAN LIFE = 65.31  
 F[X] = .60  
 X-MEAN = .349987E+01  
 STANDARD DEVIATION OF X = .749888E+00  
 STAN. DEV. OF X--SQUARED = .562332E+00

TABLE IX

WEIBULL ANALYSIS OF ROLLING CONTACT FATIGUE TESTS:

WEIBULL PLOT: 792KSI: MIL-L-7808

TEST RIG / HEAD ===== 3.4  
 TYPES OF MATERIAL ===== AS RECEIVED  
 PIN NUMBER ===== G  
 DISK OR BALL LOT NUMBER ===== 501  
 TEST OIL ===== 0-79-16  
 DATE ===== 25 FEB 85  
 NUMBER OF TESTS ===== 7  
 TOTAL NUMBER OF FAILURES ===== 7

ORDER NUMBER	MEDIAN RANK	FAILED SPECIMEN	X VALUE	Y VALUE
1	.09428	2.99	+10.95E-01	-2.31E+00
2	.22952	3.15	+11.47E-01	-1.34E+00
3	.36476	4.08	+14.06E-01	-7.90E-01
4	.50000	4.54	+15.13E-01	-3.67E-01
5	.63524	4.64	+15.35E-01	+8.48E-03
6	.77048	4.70	+15.48E-01	+3.86E-01
7	.90572	6.76	+19.11E-01	+8.59E-01

SPECIMEN LIFE VALUES WITH 90% CONFIDENCE BANDS:

		LOWER BAND	UPPER BAND
L(10) LIFE =	2.67	1.62	4.19
L(50) LIFE =	4.43	3.58	5.48

WEIBULL SLOPE	=	3.7033
CORRELATION COEFFICIENT	=	.80757
CHARACTERISTIC LIFE	=	4.90
MEAN LIFE	=	4.42
F[X]	=	.50
X-MEAN	=	.145071E+01
STANDARD DEVIATION OF X	=	.274626E+00
STAN. DEV. OF X--SQUARED	=	.754195E-01

TABLE X

WEIBULL ANALYSIS OF ROLLING CONTACT FATIGUE TESTS:

WEIBULL PLOT: 792KSI: MIL-L-7808

TEST RIG / HEAD ===== 3.4  
 TYPES OF MATERIAL ===== M50  
 PIN NUMBER ===== 12  
 DISK OR BALL LOT NUMBER ===== 501  
 TEST OIL ===== 0-79-16  
 DATE ===== 25 FEB 85  
 NUMBER OF TESTS ===== 7  
 TOTAL NUMBER OF FAILURES ===== 7

ORDER NUMBER	MEDIAN RANK	FAILED SPECIMEN	X VALUE	Y VALUE
1	.09428	10.17	+23.19E-01	-2.31E+00
2	.22952	23.74	+31.67E-01	-1.34E+00
3	.36476	32.87	+34.93E-01	-7.90E-01
4	.50000	36.12	+35.87E-01	-3.67E-01
5	.63524	36.90	+36.08E-01	+8.48E-03
6	.77048	40.51	+37.02E-01	+3.86E-01
7	.90572	49.85	+39.09E-01	+8.59E-01

SPECIMEN LIFE VALUES WITH 90% CONFIDENCE BANDS:

		LOWER BAND	UPPER BAND
L(10) LIFE =	12.18	4.71	28.83
L(50) LIFE =	32.17	21.43	48.25

WEIBULL SLOPE = 1.9402  
 CORRELATION COEFFICIENT = .81001  
 CHARACTERISTIC LIFE = 39.01  
 MEAN LIFE = 34.46  
 F[X] = .55  
 X-MEAN = .339783E+01  
 STANDARD DEVIATION OF X = .525777E+00  
 STAN. DEV. OF X--SQUARED = .276441E+00

## VOID SIZE DISTRIBUTION

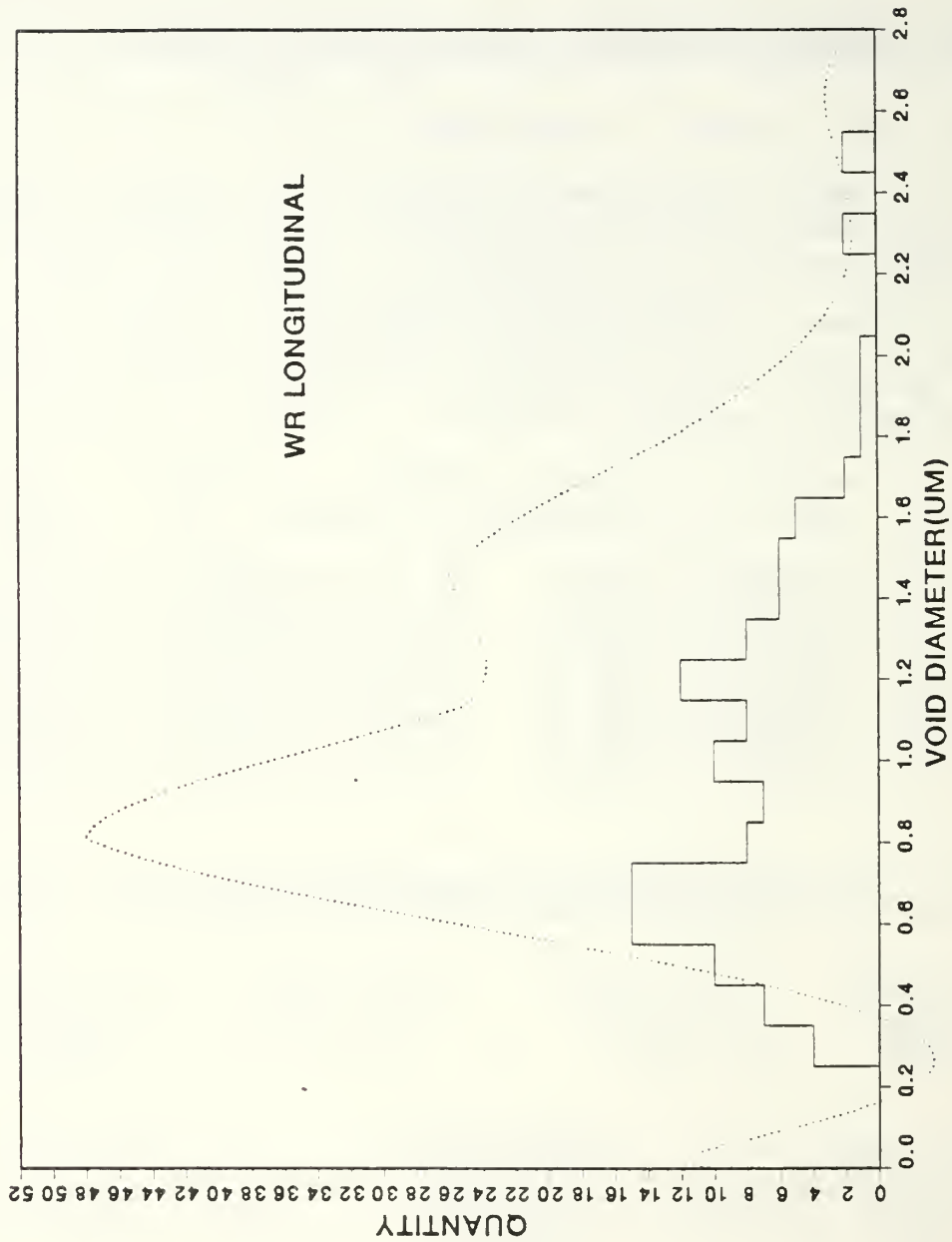


Figure C-1. Void Size Distribution of Warm-Rolled Material in the Longitudinal Direction. Histogram Represents Raw Data, Dotted Curve Represents Curve Fit Through Grouped Data.



# VOID SIZE DISTRIBUTION

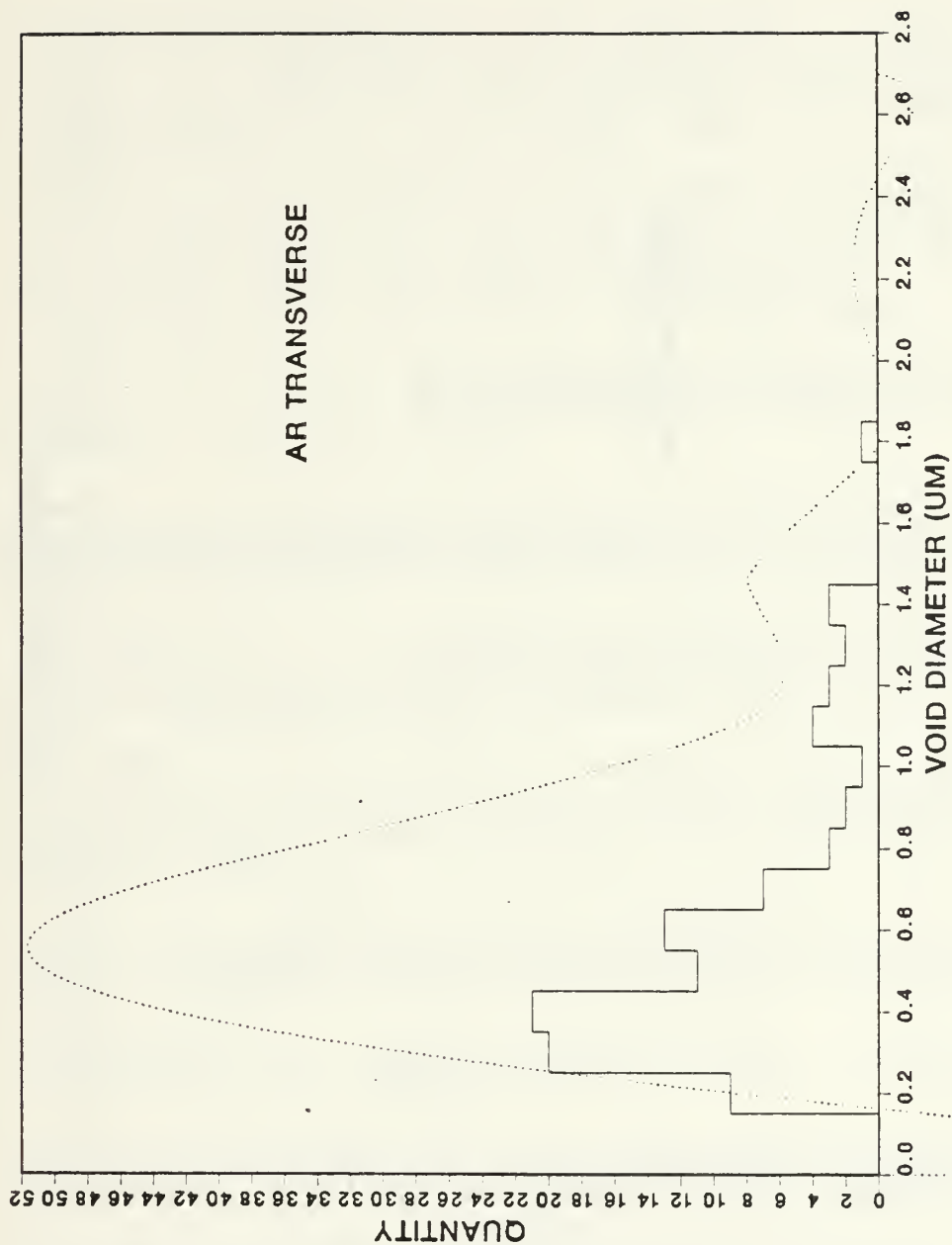


Figure C-2. Void Size Distribution of As-Received Material in the Transverse Direction. Histogram Represents Raw Data, Dotted Curve Represents Curve Fit Through Grouped Data.

# -VOID SIZE DISTRIBUTION

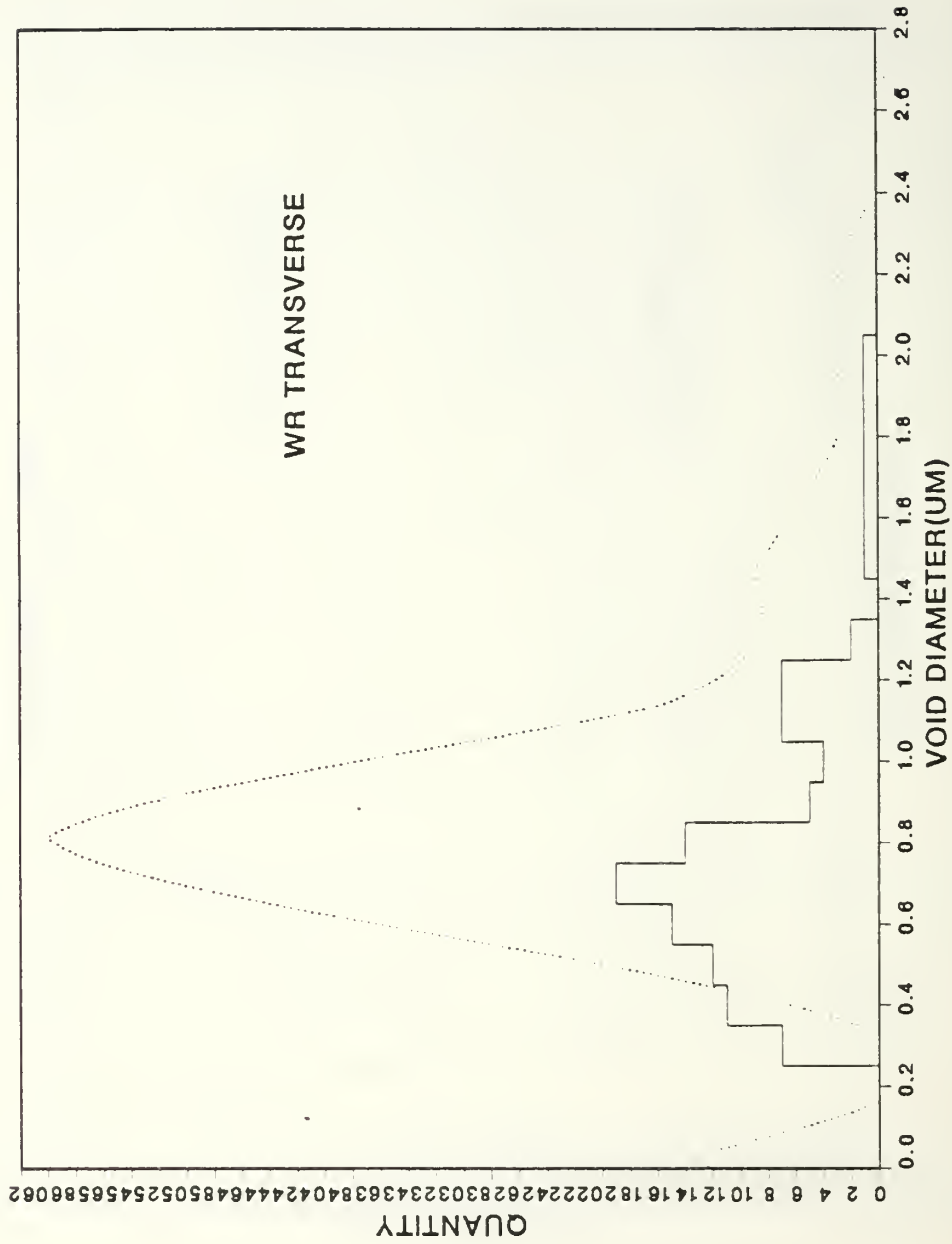


Figure C-3. Void Size Distribution of Warm-Rolled Material in the Transverse Direction. Histogram Represents Raw Data, Dotted Curve Represents Curve Fit Through Grouped Data.

## LIST OF REFERENCES

1. Sherby, O. D., Harrigan, M. J., Chamagne, L., and Sauve, C., "Development of Fine Spheroidized Structures by Warm Rolling of High Carbon Steels," Metallurgical Transactions, v. 62, pp. 575-580, 1969.
2. McNelley, T. R., Edwards, M. R., Doig, A., Boone, D. H., Schultz, C. W., "The Effects of Prior Heat Treatments on the Structure and Properties of Warm-Rolled AISI 52100 Steel," Metallurgical Transactions, v. 14A, pp. 1427-1423, July 1983.
3. Larson, K. R., Jr., Thermomechanical Processing of M-50 Steel, M.S. Thesis, Naval Postgraduate School, Monterey, California, 1983.
4. Bres, E. V., The Heat Treatment Response of Thermo-mechanically Processed M-50 Steel, M.S. Thesis, Naval Postgraduate School, Monterey, California, 1983.
5. Butterfield, F. A., Rolling Contact Fatigue Testing of Thermomechanically Processed M-50 Steel, M.S. Thesis, Naval Postgraduate School, Monterey, California, 1984.
6. Popgoshev, D. and Valori, R., "Rolling Contact Fatigue Evaluation of Advanced Bearing Steels," Rolling Contact Fatigue Testing of Bearing Steels, ASTM STP 771, pp. 342-357, 1982.
7. Glover, D., "A Ball-Rod Rolling Contact Fatigue Tester," Rolling Contact Fatigue Testing of Bearing Steels, ASTM STP 771, pp. 107-124, 1982.
8. Underwood, E. E., Quantitative Stereology, Addison-Wesley Publishing Company, 1970.
9. Johnson, L. G., The Statistical Treatment of Fatigue Experiments, Elsevier Publishing Company, 1964.
10. Camerino, N., Effect of Prior Warm Rolling on the Retained Austenite Content and Hardening Response of (VIM-VAR) AISI M-50 Steel, M.S. Thesis, Naval Postgraduate School, Monterey, California, 1985.
11. Averbach, B. L., "Fracture of Bearing Steels," Metal Progress, pp. 19-24, December 1980.

12. Tallian, T. E., "A Unified Model for Rolling Contact Life Prediction," Journal of Lubrication Technology, v. 104, pp. 336-345, July 1982.
13. Wu, E. M., Naval Postgraduate School, Monterey, California, private communication, 1985.
14. DeHoff, R. T. and Rhines, F. N., eds., Quantitative Microscopy, McGraw-Hill Bookd Company, 1968.
15. Bridge, J. E., Maniar, G. N., Philip, T. V., "Microstructural Changes on Austenitizing and Tempering of M-50 High Speed Steel," IMS Proceedings, pp. 29-40, 1970.
16. Vincent, L., Coquillet, B., and Guiraldeng, P., "Fatigue Damage of Ball Bearing Steel: Influence of Phases Dispersed in the Martensite Matrix," Metallurgical Transactions, v. 11A, pp. 1001-1006, June 1980.
17. NASA Technical Note NASA TN D-6156, Fatigue Lives at 600F of 120-Millimeter-Bore Ball Bearings of AISI M-50, AISI M-1, and WB-49 Steels, by E. N. Bamberger and E. V. Zaretsky, March 1971.



# INITIAL DISTRIBUTION LIST

	<u>No. Copies</u>
1. Defense Technical Information Center Cameron Station Alexandria, Virginia 22314	2
2. Library, Code 0142 Naval Postgraduate School Monterey, California 93943	2
3. Department Chairman, Code 69 Department of Mechanical Engineering Naval Postgraduate School Monterey, California 93943	1
4. Dr. T. R. McNelley, Code 69Mc Department of Mechanical Engineering Naval Postgraduate School Monterey, California 93943	5
5. Commander (Attn: Dan Popgoshev) Naval Air Propulsion Center P.O. Box 7176 Trenton, New Jersey 08628	2
6. Commander (Attn: Ron Dayton) Air Force Wright Aeronautical Laboratories Wright-Patterson Air Force Base Dayton, Ohio 45433-6563	2
7. LT J. L. Perry Military Sealift Command, Far East FPO Seattle 98760-2600	2
8. LCDR Mark S. Ohare 107 Peyton Drive Chicago Hgts., Illinois 60411	1









42950

Thesis

P34224

Perry

c.1

The character of  
observed porosity and  
its possible effects  
on rolling contact  
fatigue life of M-50  
steel.

42950

Thesis

P34224

Perry

c.1

The character of  
observed porosity and  
its possible effects  
on rolling contact  
fatigue life of M-50  
steel.



The character of observed porosity and i



3 2768 000 61124 8

DUDLEY KNOX LIBRARY